Ocean Engineering 243 (2022) 110322

Contents lists available at ScienceDirect

Ocean Engineering

journal homepage: www.elsevier.com/locate/oceaneng

Annual and seasonal trend detection of significant wave height, energy period and wave power in the Mediterranean Sea

Tommaso Caloiero [a,*], Francesco Aristodemo [b], Danilo Algieri Ferraro [b]

[a] National Research Council of Italy – Institute for Agricultural and Forest Systems in the Mediterranean (CNR-ISAFOM), Rende, CS, Italy
[b] University of Calabria – Department of Civil Engineering (DINCI), Rende, CS, Italy

ARTICLE INFO

Keywords:
Trend analysis
Wave height
Energy period
Wave power
Mediterranean sea

ABSTRACT

An analysis of a 40-year long wave time series was carried out in the Mediterranean basin to identify ongoing trends of three wave parameters: significant wave height, energy period and wave power. Synthetic wave data were deduced from the global atmospheric reanalysis ERA-Interim by the ECMWF. After a preliminary data examination, a trend analysis, at annual and seasonal scales, was performed on the mean and maximum values through the Mann-Kendall test. Moreover, the application of the Theil-Sen estimator allowed us to quantify the magnitude of the increase/decrease in the wave parameters. Results highlighted different behaviours between the mean and the maximum values. In general, an overall increase in the mean wave quantities was observed, particularly for the energy period, while the increase in the maximum wave parameters was limited to a few grid points. For both the mean and the maximum values, negative trends were identified in specific areas of the Mediterranean Sea, especially for the significant wave height and the wave power. The study findings could be useful for analyses linked to various activities such as coastal inundations and erosions, the design of marine structures and the identification of optimal sites for field installations of Wave Energy Converters.

1. Introduction

The Mediterranean is characterized by several human activities, which have led to strong urbanization and tourism, particularly near the coastal zones. At the same time, this area is frequently exposed to natural hazards such as earthquakes, volcano eruptions, floods, sea storms, fires and drought. As a result, several new challenges from climate change arise, involving warming, severe droughts, changing extreme events and ocean acidification (e.g. Cramer et al., 2018). The fifth report of the International Panel on Climate Change (IPCC, 2013) has underlined that the Mediterranean is one of the most vulnerable areas in the world to the impacts of global warming. Indeed, due to a strong variability of climatic variables, such as mean surface air temperature and precipitation, the Mediterranean Sea is considered a hot-spot for climate change effects (e.g., Giorgi, 2006).

In this context, the marine parameters are largely influenced by climatic changes at different spatial scales (Weisse and von Storch, 2010). Several physical processes of interest for coastal engineering are significantly affected by climate change. These include storm surges (Wang et al., 2008), sea level rises (Dasgupta and Meisner, 2009) and variations of the frequency and direction of extreme wind and wave events (González-Alemán et al., 2019) that lead to the increase in wave phenomena like run-up (Xu and Perrie, 2012) and overtopping (Chini and Stansby, 2012). Moreover, the change of wave parameters can influence the coastal erosion processes (Martins et al., 2017), the design and survivability of ships and marine structures (e.g., Foti et al., 2020) and, more recently, the performances of Wave Energy Converters (WECs) (Sierra et al., 2017; Aristodemo and Algieri Ferraro, 2018; Reguero et al., 2019).

In this last context, it is expected that, over the next years, wave energy conversion will be subject to a significant advance in research, design and field testing due to the increasing demand of renewables in energy supply (Sierra et al., 2017). Then, the knowledge of trends of the wave power can have a strong influence in addressing future economic investments in this field. To assess the wave energy potential at various locations in the world, the majority of studies in literature aimed to evaluate the yearly and seasonal mean wave power (e.g., Clément et al., 2002; Gunn et al., 2012; Vicinanza et al., 2013). However, this kind of approach does not give a realistic performance of a marine site to provide an installation of wave farms, since the analysis of the temporal

* Corresponding author. National Research Council of Italy – Institute for Agricultural and Forest Systems in the Mediterranean (CNR-ISAFOM), Via Cavour 4/6, 87036, Rende, CS, Italy.
E-mail address: tommaso.caloiero@isafom.cnr.it (T. Caloiero).

https://doi.org/10.1016/j.oceaneng.2021.110322
Received 14 November 2020; Received in revised form 19 October 2021; Accepted 4 December 2021
Available online 11 December 2021

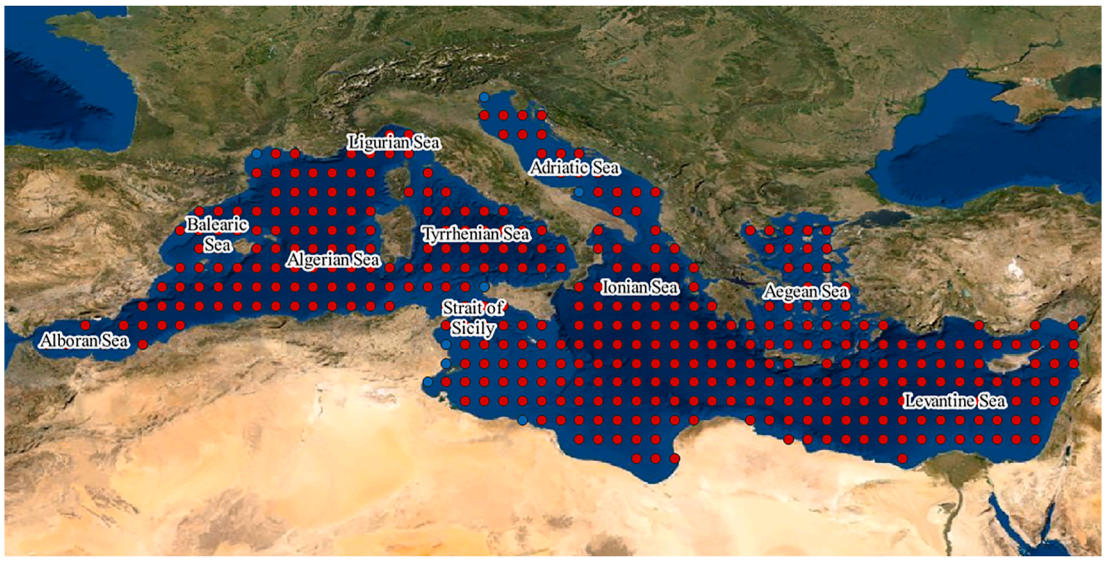

Fig. 1. Map of Mediterranean Sea with the location of ECMWF wave nodes.

variability of the wave energy resource is lacking. As pointed out by some authors (Neill and Hashemi, 2013; Reguero et al., 2015; Guillou and Chapalain, 2020), the inter-annual and seasonal variability of the wave power strongly influences the site selection, with potential negative consequences for the performance of WECs and their economic feasibility. As a result, the exploitable resource of less energetic sites having a small temporal variability proves to be comparable with most energetic ones having a large temporal variability (Portilla et al., 2013; Besio et al., 2016).

1.1. Wave trends in the world

The effects of climate change on marine areas can be used through long-term records of sea states, and to obtain a reliable trend analysis in a specific area, more than 30 years of wave recordings are needed (e.g., Shanas and Kumar, 2015). Notably, wave data are less diffused with respect to extensive datasets of land variables such as rainfall, temperature, vapour and cloud, which were regularly collected since the beginning of the past century (e.g., Mitchell and Jones, 2005). In any case, wave climate variability and trends have been widely investigated for various seas of the world though the use of different wave databases. Zikra et al. (2016) focused their attention on the trends in monthly significant wave heights, H_s, in Indonesia seas. Vanem and Walker (2013) investigated long-term trends in the time series of minimum, mean and maximum H_s values for an area of the North Atlantic Sea at different time scales. Kumar et al. (2018) analysed trends in the annual mean H_s values in the Arabian Sea and the Bay of Bengal. With reference to the China seas, previous quantities were studied by Zheng et al. (2017), while Shi et al. (2019) focused on yearly mean trends of 99th percentile of H_s. In the work by Hithin et al. (2015), trends in the annual maximum and mean H_s values and those linked to the mean zero-crossing wave period, T_m, were analysed in the Central Arabian Sea. In the Northeast Atlantic Sea, Castelle et al. (2018) detected trends in the mean and 98th percentile of H_s values during winter season. Off the Portuguese coast, trends in the yearly extreme H_s values were studied by Muraleedharan et al. (2016). Ulazia et al. (2017) assessed trends over the Bay of Biscay in the mean H_s values, also considering the corresponding values of energy period, T_e, and wave power, P. At a global scale, Aarnes et al. (2015) investigated the H_s trend at annual and monthly scale, highlighting a positive trend in mean wave conditions in the tropical ocean zones, and null trend or a slightly negative trend in the northern parts of the Pacific and Atlantic Oceans.

1.2. Wave trends in the Mediterranean Sea

Regarding the Mediterranean Sea, the object of the present study, some trend analyses have been carried out. Musić and Nicković (2008) detected trends at yearly scale of the 50th, 90th and 99th percentile of H_s in the Eastern Mediterranean between 1958 and 2001, through the use of the wave model WAM forced by the atmospheric model REMO. In particular, overall decreasing trends were observed, while for the Aegean Sea and near the coasts of Libya and Egypt, slightly positive trends in the 90th and 99th percentile were noticed. Martucci et al. (2010) performed a trend modeling of average and extreme H_s values for some points belonging to the Italian seas in the period 1958–1999 adopting the WAM forced by the ERA-40 dataset. The authors highlighted the existence of an initial negative trend in H_s and successive positive trends, i.e. after a turning point in the late 80s. For the whole Mediterranean Sea and using satellite measurements, Young et al. (2011) analysed the yearly mean of the 90th and 99th percentile of H_s, obtaining an overall positive trend in the 1985–2008 time window. Casas-Prat and Sierra (2013) carried out a trend analysis during summer and winter in the area involving the Balearic Sea and the Gulf of Lion, taking into account the mean and extreme values of H_s, peak period, T_p, and mean wave direction, θ. Through the use of five combinations of global-regional circulation models, this analysis showed a maximum rate of projected changes of around ±10% for mean conditions versus ±20% for extreme climate. In a recording station of the northern Adriatic Sea, Pomaro et al. (2017) studied H_s trends between 1979 and 2015, highlighting an evident decrease in the highest percentile (99th) and a smaller increase in the 50th and 75th ones. Along the Calabrian coast belonging to the southern Italy, Caloiero et al. (2019) detected slightly positive trends in the yearly and seasonal mean values of H_s and relevant positive trends in those related to T_e on the basis of a 39-year-long time series deduced from ERA-Interim wave database. The same dataset was used by Caloiero and Aristodemo (2021) to detect trends of yearly and seasonal mean values of H_s, T_e and P along the Italian seas, showing overall positive trends particularly for T_e, mainly in the Ionian and Tyrrhenian seas, and a higher percentage of variability during seasons when compared to the annual analysis. Lastly, De Leo et al. (2020) analysed trends over the Mediterranean basin for maxima, 98th percentile and mean H_s at yearly scale using 40 years of numerical hindcast of sea states, evidencing a different trend behaviour between mean and extreme values.

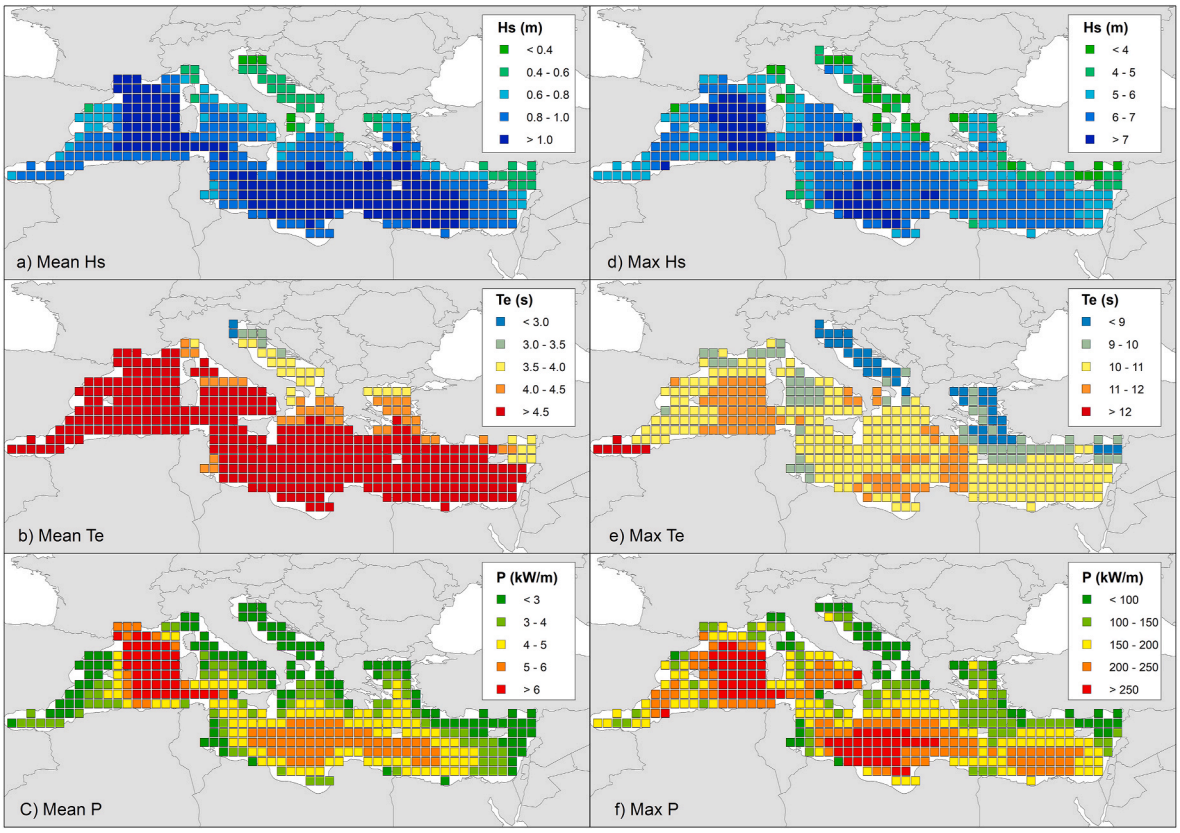

Fig. 2. Characterization of the mean annual values of (a) H_s (b) T_e and (c) P and of the maximum annual values of (d) H_s (e) T_e and (f) P through boxplots.

1.3. Aims of the work and organization of the sections

The objective of the present investigation is to detect and quantify possible trends in the significant wave height over the Mediterranean basin, by considering, the energy period and the wave power for the first time. This study aims to analyze the trends of the wave power, P, and the wave parameters, H_s and T_e, included in its calculation. The mean and maximum values of H_s, T_e and P have been analysed at seasonal and annual scales.

The present paper is organised as follows. In Section 2, the interest zone and the input wave data are briefly presented. The adopted methodologies, with reference to the evaluation of the wave power and the approaches to perform the trend analysis, are described in Section 3. The mean and maximum wave parameters are firstly assessed in the Mediterranean basin, and then a trend analysis at yearly and seasonal scales is performed in Section 4. In Section 5 a comparaison between the current trend results with those obtained by previous studies is carried out. The last section presents the conclusions.

2. Interest zone and input wave data

The Mediterranean Sea is connected to the Atlantic Ocean through the Strait of Gibraltar and is substantially enclosed by land: on the north by Southern Europe and Anatolia, on the south by North Africa, on the east by the Levant and on the west by Spain and France. It covers an area of about 2.5 million of km^2, representing 0.7% of the global ocean surface. Placed between 30° and 46° N and 6° W and 36° E, it shows a west-east length of about 4000 km with mean and maximum water depths of 1430 m and 5121 m, respectively.

In this work, the wave data related to H_s and T_e in the period 1979–2018 were obtained from the global atmospheric reanalysis ERA-Interim by the ECMWF, for a total of 40 years, a spatial resolution of 0.75° × 0.75° and time sampling of 6 h. Fig. 1 shows the adopted 417 wave nodes in the Mediterranean basin, with the classification of the principal marginal seas. In particular, red points refer to wave nodes in deep water conditions (98.1% of the total ones), while blue points are associated with wave nodes that can occur in deep or intermediate water conditions (1.9% of the total ones). The involved ECMWF nodes are placed at water depths oscillating between 17.7 m and 4441.7 m.

3. Methodology

3.1. Estimate of wave parameters

The wave quantities representing sea states used in the present work are H_s and T_e. In addition, the wave power per unit crest length, P, depending on H_s and T_e, is also taken into account.

Using the spectral analysis, the value of H_s is equal to:

$$H_s = 4\sqrt{m_0} \tag{1}$$

where m_0 is the zero-th spectral moment that is determined as:

$$m_0 = \sum_{ij} S_{ij} \Delta f_i \Delta \theta_j \tag{2}$$

in which S_{ij} is the density over the i-th frequency and j-th direction, Δf_i is the i-th frequency width of the density and $\Delta \theta_i$ is the j-th angular width of the density.

The value of T_e, which represents the variance-weighted mean period of the one-dimensional density spectrum, is given by the following equation:

$$T_e = \frac{m_{-1}}{m_0} \tag{3}$$

being m_{-1} the minus-one spectral moment due to:

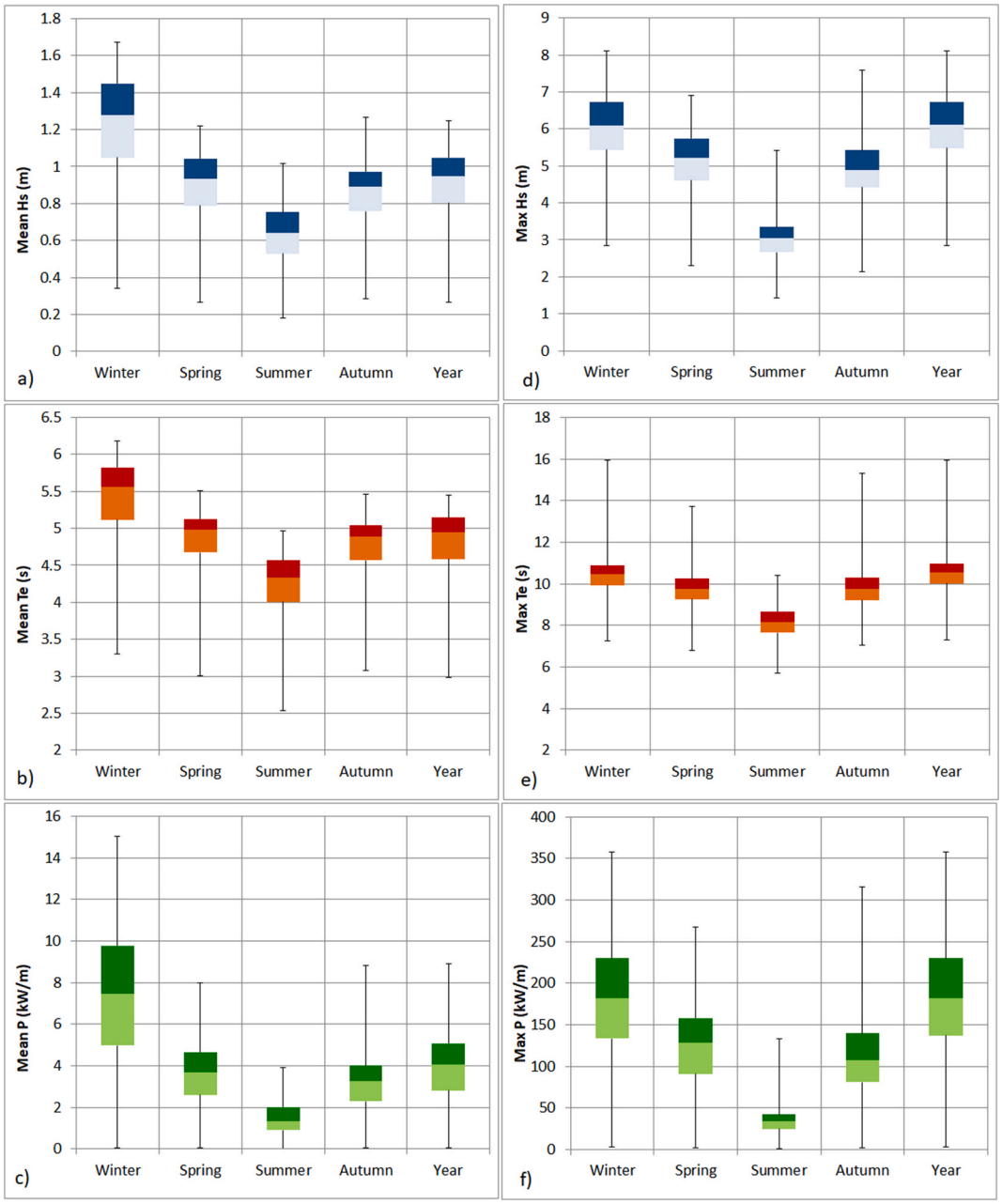

Fig. 3. Spatial distribution of the mean annual values of (a) H_s (b) T_e and (c) P and of the maximum annual values of (d) H_s (e) T_e and (f) P.

$$m_{-1} = \sum_{ij} f_i^{-1} S_{ij} \Delta f_i \Delta \theta_j \tag{4}$$

where f_i is the i-th frequency.

The value of P is determined by the following general expression adopted for all water conditions (i.e. from deep to shallow):

$$P = E c_g \tag{5}$$

where E is the wave energy expressed as:

$$E = \frac{\rho g}{16} H_s^2 \tag{6}$$

where ρ (density of salt water) $\approx$ 1025 kg/m^3 and g (gravity acceleration) $\approx$ 9.806 m/s^2.

The group celerity, c_g, is given by:

$$c_g = \frac{c}{2}\left[1 + \frac{2kd}{sinh(2kd)}\right] \tag{7}$$

where c (mean celerity) $= L_m/T_e$, k (mean wave number) $= 2\pi/L_m$, d is the water depth and L_m is the mean wave length calculated by the linear dispersion relationship as:

$$L_m = \frac{gT_e^2}{2\pi} tanh(kd) \tag{8}$$

A quadratic and linear dependency of P on H_s and T_e, respectively, can be noted.

The values of H_s and T_e taken from the ECMWF dataset were subject to a processing phase in order to check their consistency for the subsequent analyses. Some criteria were adopted to eliminate not physical i-th wave parameters in the following manner (Algieri Ferraro et al., 2016):

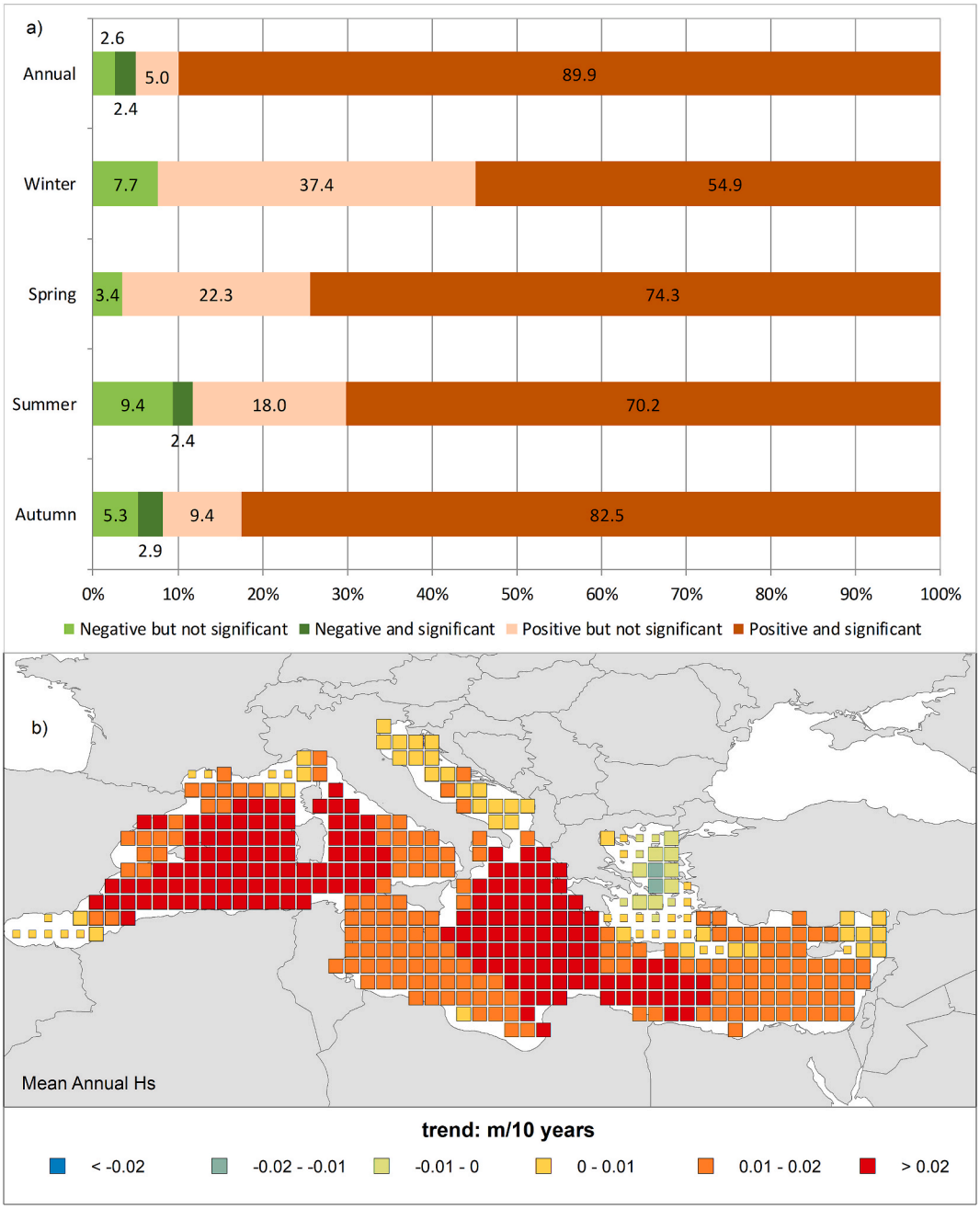

Fig. 4. (a) Seasonal and annual percentages of grid points presenting positive or negative trends in the H_s mean values and (b) spatial distribution of the annual trend of mean H_s.

- appearing of Not a Numbers, zero and repeated values;
- outlier data incompatible with their spatial location in the Mediterranean Sea, i.e. values of H_s and T_e greater than 10 m and 18 s, respectively;
- $|H_{s,i+1}\text{-}H_{s,i}| > 1.5$ m with $|\theta_{i+1}\text{-}\theta_i| < 30°$, where$\theta$ is the mean wave direction;
- $T_{p,i}/T_{e,i} > 2$, where T_p is the peak period;
- $H_{s,i}/L_{p,i} < 0.1$ (as in Miche, 1951).

where L_p (peak wave length) $= gT_p^2\tanh(kd)/(2\pi)$.

Considering all ECMWF wave nodes, the mean efficiency given by the ratio between processed data and initial ones is generally good and equal to 99.94%.

3.2. Mann-Kendall test

The possible presence of temporal tendencies in the H_s, T_e and P series has been assessed by means of two non-parametric tests. In particular, the statistical significance was assessed with the Mann-Kendall (MK) non-parametric test (Mann, 1945; Kendall, 1962).

Equation (9) shows the MK statistic S, considering the null hypothesis (H_0) that the data come from a population whose random variables are independent and identically distributed, while the alternative hypothesis (H_1) represents the existence of a monotonic trend.

$$S = \sum_{i=1}^{n-1}\sum_{j=i+1}^{n} sgn(x_j - x_i); \quad \text{with } sgn(x_j - x_i) = \begin{cases} 1 & \text{if } (x_j - x_i) > 0 \\ 0 & \text{if } (x_j - x_i) = 0 \\ -1 & \text{if } (x_j - x_i) < 0 \end{cases} \tag{9}$$

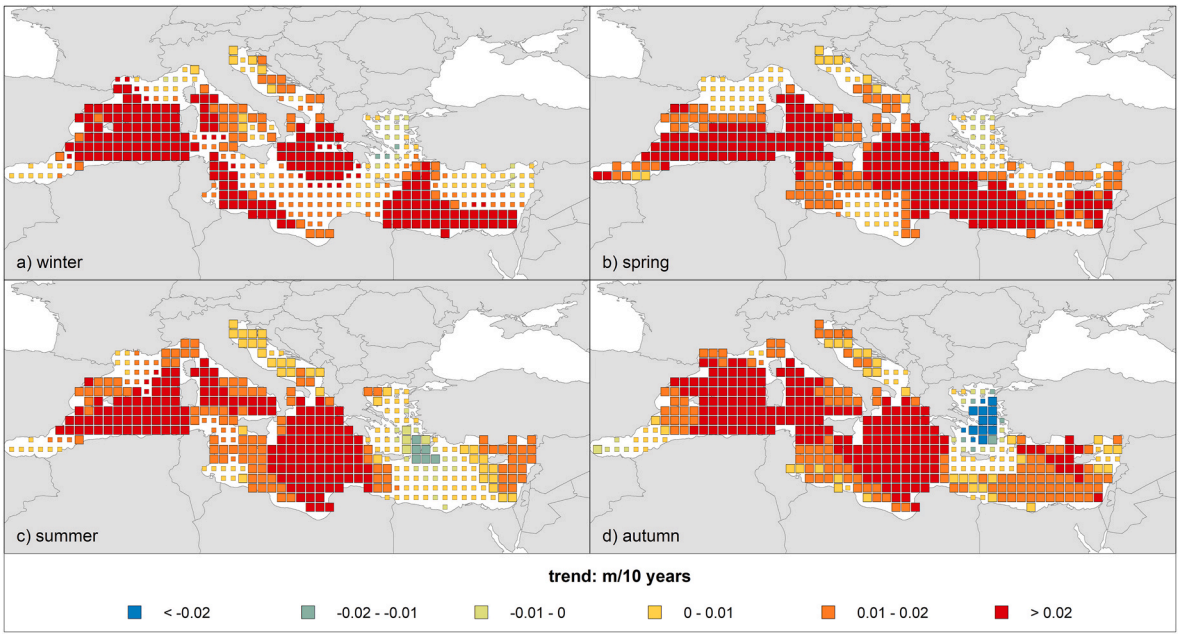

Fig. 5. Spatial distribution of the seasonal trend of the mean H_s values for (a) winter, (b) spring, (c) summer and (d) autumn.

where n is the size of the sample and *sgn* is the signal of the difference of subsequent data.

For independent and randomly ordered values, the statistic S approximates to the normal distribution, for samples with $n > 10$, with mean and variance given by:

$$E(S) = 0 \tag{10}$$

$$Var(S) = \left[n(n-1)(2n+5) - \sum_{1=1}^{p} t_i(t_i-1)(2t_i+5) \right] \Big/ 18 \tag{11}$$

where E is the mean of S, Var is the variance of S, p is the number of tied groups and t_j is the number of data of the j-order tied group.

The standardized test statistic Z_{MK} can be computed as:

$$Z_{MK} = \begin{cases} \dfrac{S-1}{\sqrt{Var(S)}} & \text{for } S > 0 \\ 0 \quad \text{for } S = 0 \\ \dfrac{S+1}{\sqrt{Var(S)}} & \text{for } S < 0 \end{cases} \tag{12}$$

By applying a two-tailed test, for a specified significance level α, the significance of the trend can be evaluated. In particular, in this work, the series of H_s, T_e and P have been examined for a significance level equal to 90%.

3.3. Theil-Sen estimator

The slopes of the trends were calculated by the Theil-Sen (TS) estimator (Sen, 1968) which has been selected because it is more powerful than linear regression methods in the trend slope evaluation in the presence of outliers in the series.

The first step in the calculation of the TS estimator is to evaluate the values of Q_i, given N pairs of data:

$$Q_i = \frac{x_j - x_k}{j-k} \text{ for }, \; i \;\; = \;\; 1, \ldots, N \tag{13}$$

in which x_j and x_k are the data values at times j and k (with $j>k$), respectively.

If there is only one datum in each time period, then $N = n(n–1)/2$, where n is the number of time periods. If there are multiple observations in one or more time periods, then $N<n(n–1)/2$, where n is the total number of observations.

The TS estimator is then computed as the median Q_{med} of the N values of Q_i, ranked from the smallest to the largest:

$$Q_{med} = \begin{cases} Q_{[(N+1)/2]} & \text{if } N \text{ is } odd \\ \dfrac{Q_{[N/2]} + Q_{[(N+1)/2]}}{2} & \text{if } N \text{ is } even \end{cases} \tag{14}$$

The Q_{med} sign reveals the trend behaviour, while its value indicates the magnitude of the trend.

4. Results

4.1. Wave climate analysis

After the quality check of the ECMWF data, an assessment on the wave climate in the Mediterranean Sea was carried out through the 417 grid series of H_s and T_e and the obtained values of P by Eq. (5). This preliminary analysis proves to be useful to match the mean and maximum wave parameters with the projections obtained by the trend analysis.

Fig. 2 highlights the spatial distribution of the mean and maximum H_s, T_e and P series in the Mediterranean basin at yearly scale. Specifically, all the left subplots refer to the mean values, while all the right subplots refer to the maximum ones. With reference to the mean H_s series (Fig. 2a), the largest values, i.e. greater than 1 m, occurred between the Algerian Sea and the southern part of France (Gulf of Lion), in the Southern zone of the Tyrrhenian and Ionian seas and between the Aegean and Levantine seas. This spatial distribution is quite similar to that simulated using the WAM model and observed satellite data from ESA-CNES network (Lionello et al., 2008; Galanis et al., 2012). The peak of the mean H_s values is 1.26 m and was identified in the northern part of the Algerian basin. The lowest mean H_s values, i.e. less than 0.4 m, were detected in the northern areas of the Ionian and Adriatic seas. Except for few cases, close to the coasts, the mean values of H_s were smaller than those observed in the open seas. In detail, the mean value of H_s in the open seas is 0.94 m. Regarding the mean T_e values (Fig. 2b), this wave parameter showed lesser spatial variability with respect to H_s, with the greatest values, i.e. larger than 4.5 s, diffused in a large area belonging to

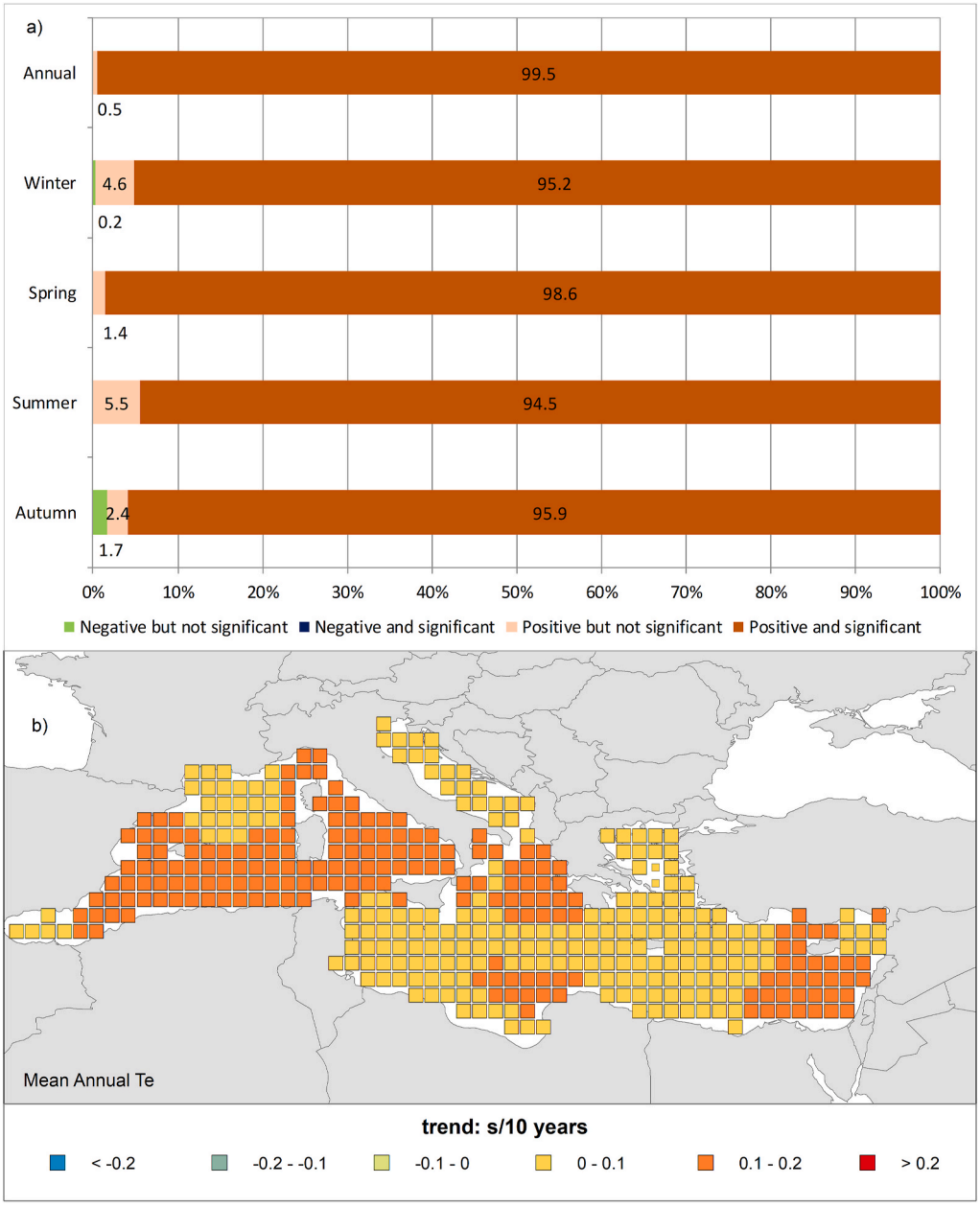

Fig. 6. (a) Seasonal and annual percentages of grid points presenting positive or negative trends in the T_e mean values and (b) spatial distribution of the annual trend of mean T_e.

the central and southern Mediterranean basin. The lowest mean T_e series were substantially identified in the Adriatic Sea, especially in its northern part, with the smallest value equal to 2.97 s located in the same node where the lowest mean H_s value occurred. Paying attention to the mean P values (Fig. 2c), their spatial variability is more relevant than the H_s and T_e ones. Average wave powers greater than 6 kW/m were concentrated between the Algerian basin and the southern part of France and close to the Strait of Sicily, with a peak value of 9.16 kW/m individuated in the northern part of the Algerian Sea. The lowest P values, i.e. less than 3 kW/m, were detected in the Balearic, Ligurian and Adriatic seas, and in the northern areas of the Tyrrhenian, Ionian, Aegean and Levantine seas, particularly for the grid points near the coasts. The above results on mean P values agree with the wave energy assessments for electricity purposes performed in the Mediterranean Sea by Liberti et al. (2013), Besio et al. (2016) and Vannucchi and Cappietti (2016) using other wave databases.

Concerning the spatial distribution of the maximum series, a larger variability in the data occurred when compared to the mean ones. As also observed by Lionello et al. (2008), the areas with the largest maximum values of H_s, i.e. greater than 7 m, correspond to those observed for the mean values (Fig. 2d). For example, the maximum value of H_s (8.59 m) has been identified in the northern part of the Algerian basin. A similar correspondence has been detected between the lowest maximum, i.e. less than 4 m, and minimum values of H_s. Indeed, except for some grid points located in the northern parts of Aegean and Levantine seas, the majority of the mentioned values were mainly detected in the northern areas of Ionian and Adriatic basins. Fig. 2e shows a different spatial distribution of the maximum T_e values than the mean ones. In fact, the highest values, i.e. larger than 12 s, were concentrated in the Alboran Sea, with a peak equal to 15.95 s, while lower values, ranging from 11 s to 12 s, were detected in the Algerian basin and between the Ionian and the Levantine seas. With respect to the spatial distribution of the maximum P (Fig. 2f), values larger than 250 kW/m occur in the Algerian Sea (maximum value of 357.3 kW/m), as in

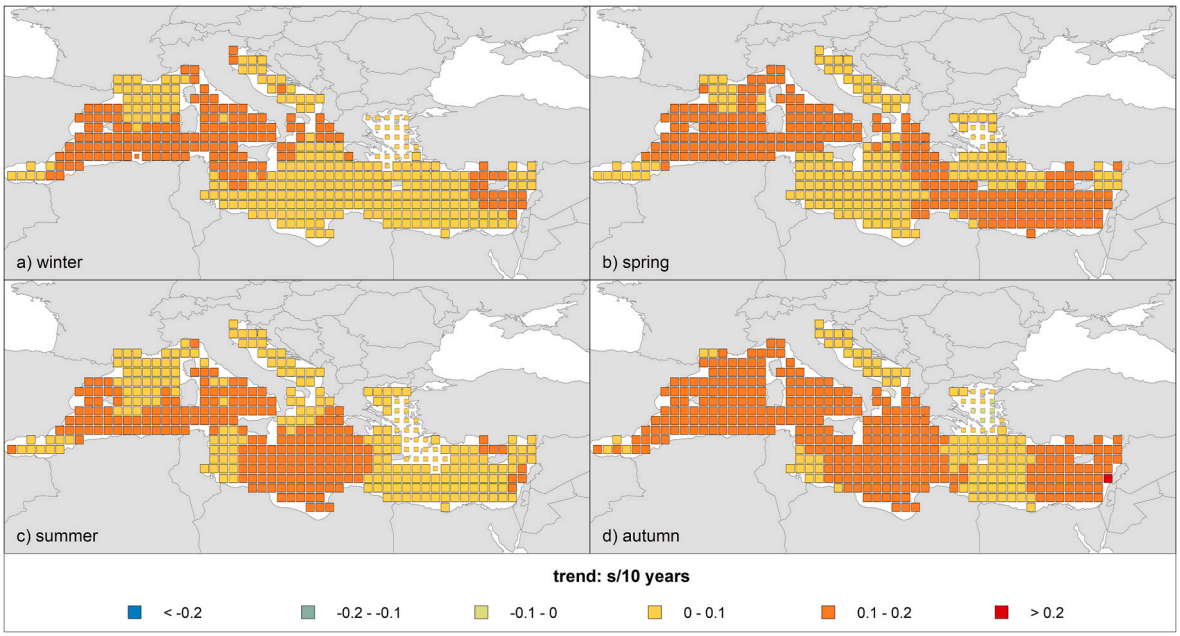

Fig. 7. Spatial distribution of the seasonal trend of the mean T_e values for (a) winter, (b) spring, (c) summer and (d) autumn.

the case of the corresponding mean values, in the Ionian Sea and in the Libyan coasts. The lowest P values, i.e. less than 100 kW/m, were observed in some parts of Ligurian, Ionian, Aegean and Levantine basins and in the Adriatic Sea.

In Fig. 3, the mean and maximum H_s, T_e and P series have been characterized at seasonal and annual scales through boxplots. The bottom and top of the box represent the second and third quartiles, the band within the box represents the median and the ends of the whiskers are the minimum and maximum of all of the wave nodes. As in Fig. 2, all the left subplots refer to the mean values, while all right subplots refer to the maximum ones. Fig. 3a, b and 3c show the seasonal and yearly mean H_s, T_e and P values, respectively. As expected, for all the variables the greatest values were observed during winter, while the lowest ones were identified in summer. Similarly, considering the variability of the different variables, in winter and in summer the largest and the smaller variabilities have been identified, respectively. This seasonal behaviour could be linked to the climate of the Mediterranean basin and, in particular, to the local wind patterns and the magnitude of the marginal Seas, i.e., the extension of the fetches. In fact, the western Mediterranean basin is exposed to different strong winds (i.e. the Vendaval wind from the South West of the Balearic basin, the Ponente wind from the West through the Straits of Gibraltar, the Mistral wind from the North West, the Sirocco wind from the South and South East, the Levant wind from East and North East, the Libeccio wind from South West in Corsica and the Tyrrhenian basin, the Tramontane wind from the North, and the Marin from the South West of the Gulf of Lion) whose intensity differ among the several seasons (Amarouche and Akpınar, 2021).

In particular, considering the three variables, the wave power is characterized by the greatest seasonal variability, while an opposite behaviour has been observed for the energy period. Furthermore, for all the variables, the yearly mean distributions were very close to those detected in spring. Fig. 3d, e and 3f describe the seasonal and yearly maximum H_s, T_e and P values, respectively. Also for this analysis, the largest values were detected in winter, as well as the highest variability, which occurred in this season and for the wave power. Also, the yearly maximum H_s, T_e and P values corresponded to those obtained during winter. In addition, the maximum H_s, T_e and P values during spring and autumn are similar, particularly for T_e. These results are consistent with a number of investigations conducted in shelf seas (e.g., Neill and Hashemi, 2013; Guillou and Chapalain, 2020) such as the Mediterranean Sea (Liberti et al., 2013; Besio et al., 2016).

In order to investigate the inter-annual and seasonal variability that can influence the optimal selection of a site for WEC installations, an analysis of the coefficient of variation and the seasonal variability index was carried out on the basis of the mean wave power at annual and seasonal scales (see Appendix A). Furthermore, the spatial and temporal correlations between the involved three wave parameters, i.e. H_s–T_e, H_s–P and T_e–P, have been identified through the determination of the Pearson correlation coefficient. Considering mean and maximum values of H_s, T_e and P at yearly scale, these correlations are shown in Appendix B.

4.2. Trend analysis of mean values

The results of the trend analysis applied to the annual and seasonal mean H_s values are presented in Fig. 4 and Fig. 5. In particular, Fig. 4a shows the percentages of grid points with a positive or negative trend for H_s. As a result, at annual scale, a marked positive trend was detected. In fact, about 90% of the grid points showed a positive trend, while significant negative trends were identified in only 2.4% of the grid points.

The positive trend of yearly mean H_s values is spatially distributed throughout the entire study area, with the highest increment detected in the western part of the Mediterranean basin, in front of Algeria, where the application of the Theil-Sen estimator has allowed the authors to identify an increase of more than 0.04 m/10 years (Fig. 4b). It is worth noting that, in Fig. 4b, as well as in the following Figures explaining the spatial distribution of the trends, squares dimension indicates the significance level (SL) of the trend. In particular, large squares dimension suggests a significant trend (SL = 90%), while small squares otherwise, i.e. a not significant trend. A lower increasing trend of H_s was detected in the central zone of the Mediterranean Sea and the western parts of the Tyrrhenian and Levantine seas, with a magnitude greater than 0.02 m/10 year (Fig. 4b). As regards the Aegean Sea, this is the only area in the Mediterranean basin where a negative trend of the annual mean H_s values was identified, with a maximum reduction of −0.016 m/10 years (Fig. 4b).

As shown in Fig. 4a, the trend analysis performed at seasonal scale confirmed the results obtained at annual scale, with a marked positive trend of the mean H_s values, even though with a different behaviour from season to season. In winter, about 55% of the grid points showed

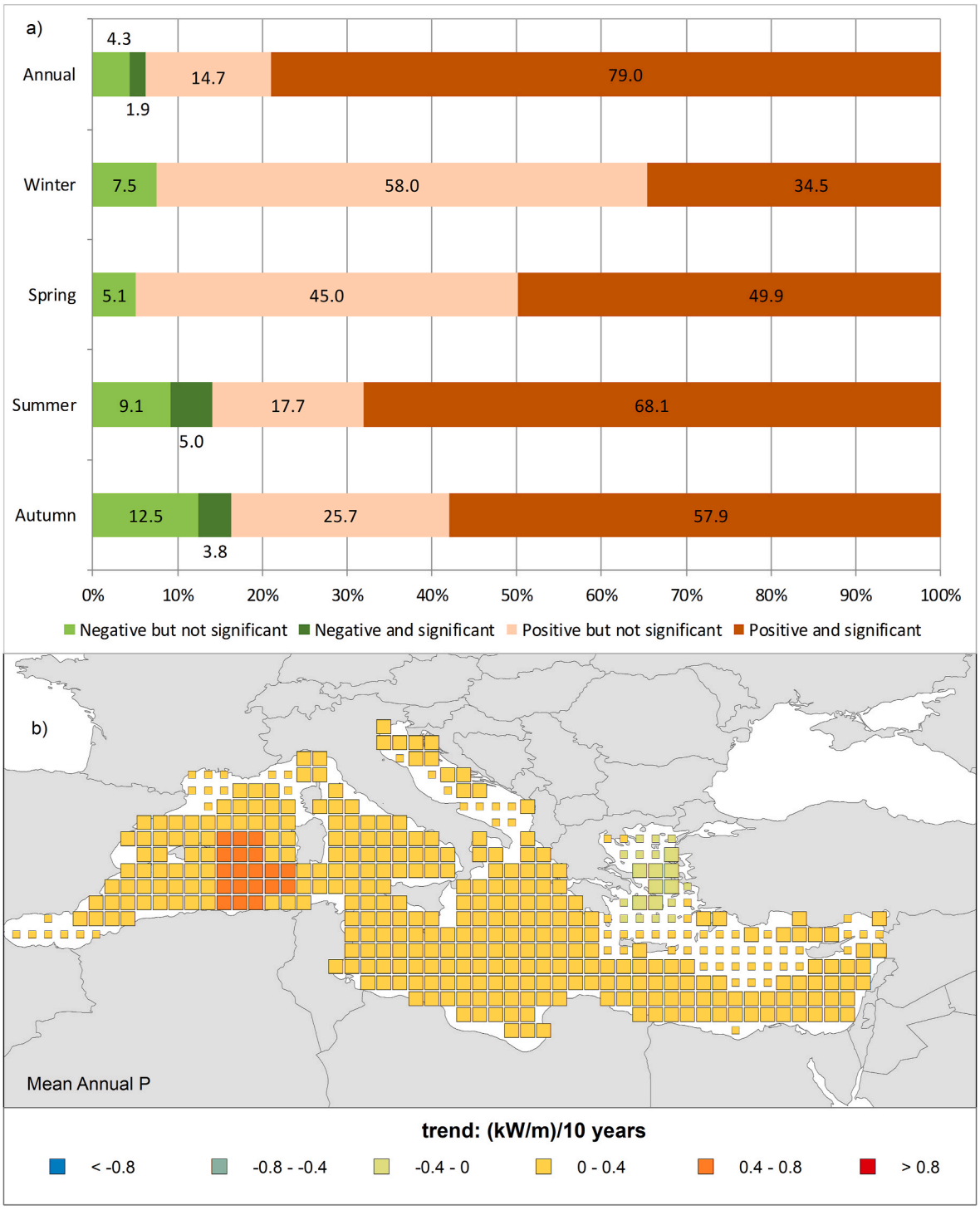

Fig. 8. (a) Seasonal and annual percentages of grid points presenting positive or negative trends in the *P* mean values and (b) spatial distribution of the annual trend of mean *P*.

significant positive trends. Similarly, in spring only significant positive trends were obtained, involving more than 74% of the grid points. Conversely, in summer and in autumn both positive (more than 70% and 80% of the grid points, respectively) and negative (2.4% and 2.9% of the grid points, respectively) trends of the mean H_s values were detected.

As regards the seasonal analysis, Fig. 5 shows the spatial distribution of the results in the Mediterranean Sea, confirming different trend behaviours of H_s in the several seasons. In fact, during winter (Fig. 5a) positive trend values of H_s were mainly detected in the Algerian, Tyrrhenian and Levantine basins, with increases of more than 0.06 m/10 years, more than 0.03 m/10 years and more than 0.02 m/10 years, respectively. During spring, relevant positive trends (more than 0.03 m/10 years) were identified in the southern part of the Algerian basin and in the Ionian basin (Fig. 5b). In summer, the trend behaviour is similar to the one obtained for spring, with the highest values (more than 0.04 m/10 years) detected in both the southern part of the Algerian basin and in the Ionian basin. Differently from the spring trend, in summer negative trends (more than −0.01 m/10 years) have been identified between the Aegean and the Levantine basins (Fig. 5c). Finally, concerning autumn, a marked positive trend (maximum magnitude equal to about 0.05 m/10

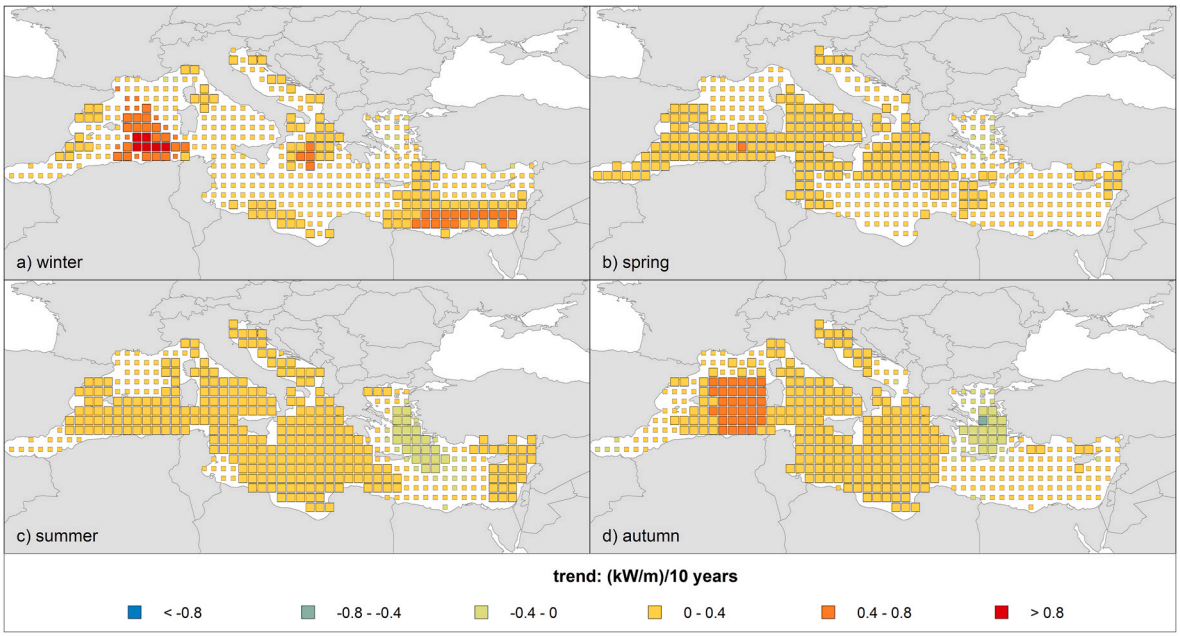

Fig. 9. Spatial distribution of the seasonal trend of the mean P values for (a) winter, (b) spring, (c) summer and (d) autumn.

years) of H_s has been highlighted with the exception of the Aegean Sea, where a negative trend was detected, with a maximum reduction of more than −0.04 m/10 years (Fig. 5d).

The trend analysis was also performed for the yearly and seasonal mean T_e values (Figs. 6 and 7). Fig. 6a highlights the percentages of wave nodes with a positive or negative trend using T_e. When compared to H_s, a marked and significant positive trend for all the temporal aggregations is evident. Specifically, at annual scale, 99.5% of the wave nodes denoted a significant positive trend.

Fig. 6b shows the spatial distribution of the trends for the yearly mean T_e values in the Mediterranean Sea. Positive trends with different magnitudes occurred in the entire studied basin. Highest positive trends of about 0.15 s/10 years appeared in the Algerian Sea, in the entire Tyrrhenian Sea and in the most part of the Ionian and Levantine seas.

The seasonal analysis of the trends applied to mean T_e values highlighted a similar behaviour of that performed at annual scale (Fig. 6a). The percentage of grid points having a significant positive trend was greater than 90% for all seasons. Specifically, percentages corresponding to 95.2%, 98.6%, 94.5% and 95.9% of the wave nodes were observed during winter, spring, summer and autumn, respectively.

Fig. 7 describes the spatial variation of the seasonal trend analysis on the mean T_e values in the Mediterranean Sea. For all the seasons, positive trends occurred in almost all areas of the Mediterranean Sea, except for some nodes in the Aegean Sea where no trends were observed. In particular, during winter (Fig. 7a), a maximum positive trends of T_e of more than 0.17 s/10 years was observed in the Algerian Sea. The spatial trend behaviour in spring (Fig. 7b) is similar to the winter one (Fig. 7a), with the exception of a higher concentration of positive trends in the Ionian and Levantine basins. The greatest increment is equal to 0.18 s/10 years and located in the Balearic Sea. During summer (Fig. 7c), positive trends were mainly detected in the Algerian and Tyrrhenian seas and in the Southern area of the Ionian Sea, with a maximum increase of 0.17 s/10 years occurring in the Tyrrhenian one. In the last analysed season, i.e. autumn, a significant percentage of grid points showed positive trends with a magnitude ranging from 0.1 s to 0.2 s/10 years, especially in the Algerian, Balearic, Tyrrhenian and Ionian seas and the eastern part of the Levantine Sea where a magnitude slightly greater than 0.2 s/10 years has been identified (Fig. 7d).

Fig. 8 and Fig. 9 describe the results of the trend analysis performed on the yearly and seasonal mean P values. In particular, Fig. 8a shows the percentages of grid points with a positive or negative trend considering P. Owing to the quadratic dependency on H_s and the linear dependency on T_e, there is a prevalence of positive trends for this involved quantity. In fact, at annual scale, 79% of the grid points highlighted a positive trend, while a percentage of 1.9% of the grid points denoted a negative trend.

Fig. 8b shows the spatial distribution of the trends for the yearly mean P values in the Mediterranean basin. As a result, a marked percentage of wave nodes with positive trends has been observed, with a maximum value equal to 0.53 kW/m/10 years identified in the Algerian Sea. Negative trends occurred in the central part of the Aegean Sea with a maximum magnitude equal to −0.12 kW/m/10 years.

At seasonal scale, the percentage of wave nodes presenting a significant trend decreases with respect to the annual scale (Fig. 8a). Specifically, significant positive trends associated to winter, spring, summer and autumn occurred in 34.5%, 49.9%, 68.1% and 57.9% of the wave nodes, respectively. Significant negative trends appeared only in summer and autumn with a percentage equal to 5% and 3.8%, respectively.

Fig. 9 illustrates the spatial variation of the trends for the seasonal mean P values in the Mediterranean Sea. As a result, a relevant spatial variation of the trends during the four seasons was obtained. In winter (Fig. 9a), the highest positive trends were identified in the Algerian Sea, reaching a maximum value slightly larger than 1 kW/m/10 years. During spring (Fig. 9b), the spatial distribution of the trend evaluated for mean P values was characterized by a prevalence of positive values oscillating from 0 to 0.4 kW/m/10 years and mainly concentrated in the Balearic, Algerian, Tyrrhenian and Ionian seas. In summer (Fig. 9c), a dominance of positive trends oscillating between 0 and 0.4 kW/m/10 years, principally distributed in the central part of the Mediterranean basin, has been highlighted. A maximum trend magnitude of 0.24 kW/m/10 years has been identified in the Ionian Sea. Between the Aegean and Levantine seas, some wave nodes showed negative trends, with a maximum value equal to −0.14 kW/m/10 years. Similarly to spring and summer, during autumn (Fig. 9d) positive trends characterized the most part of the wave nodes, mainly in the Adriatic, Tyrrhenian and Ionian seas and especially in the Algerian Sea, with the greatest value equal to 0.64 kW/m/10 years. Similarly to summer, negative trends occurred in the Aegean Sea, where one wave node showed the greatest negative trend in this season, namely −0.47 kW/m/10 years.

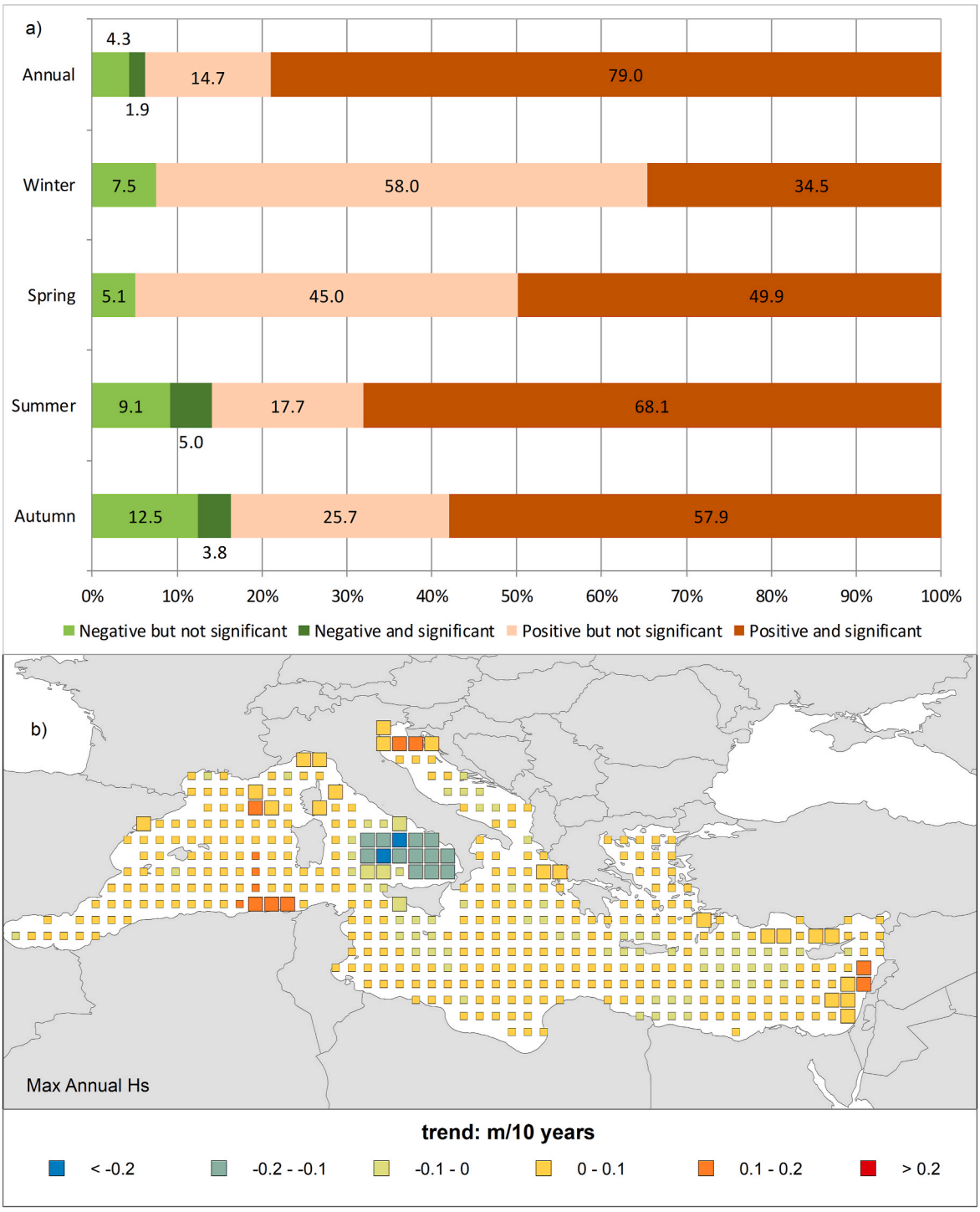

Fig. 10. (a) Seasonal and annual percentages of grid points presenting positive or negative trends in the H_s maximum values and (b) spatial distribution of the annual trend of maximum H_s.

4.3. Trend analysis of maximum values

Concerning the yearly and seasonal maximum H_s values, the obtained results of the trend analysis are shown in Fig. 10 and Fig. 11, respectively. Fig. 10a shows the percentages of wave nodes having positive or negative trends. At yearly scale, a strong reduction of significant positive trends was noticed in comparison with the mean values, leading to a percentage limited to 7% of the grid points. As in the case of the mean H_s values, the percentage of significant negative trends of the maximum H_s values was lower than the positive one and equal to 4.3% of the wave nodes.

The spatial distribution of the trend analysis performed on the yearly maximum H_s values is shown in Fig. 10b. In this case, the highest positive trends were substantially observed in the Algerian, Adriatic and Levantine seas, with a maximum value equal to 0.18 m/10 years detected in the Algerian one. Negative trends were concentrated in the Tyrrhenian Sea, with an extreme value corresponding to −0.24 m/10 years.

The trend analysis carried out at seasonal scale showed a general increase in significant positive trends of the maximum H_s values when

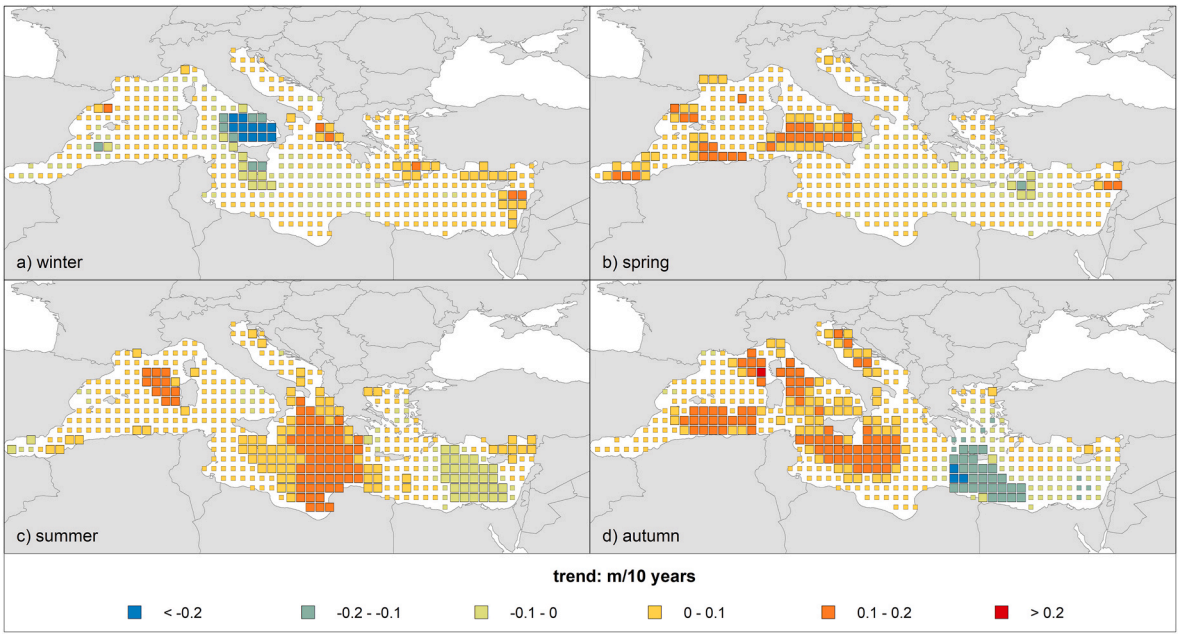

Fig. 11. Spatial distribution of the seasonal trend of the maximum H_s values for (a) winter, (b) spring, (c) summer and (d) autumn.

compared to the annual ones, particularly in summer and autumn (Fig. 10a). In fact, the percentages of significant positive trends reached values equal to 7.6%, 15.9%, 33.3% and 31.8% of the grid points during winter, spring, summer and autumn, respectively. Significant negative trends were observed for a percentage of grid points oscillating between 1.7% (spring) and 7.9% (summer).

The spatial results of the trend analysis on the seasonal maximum H_s values are illustrated in Fig. 11. In general, a relevant spatial variability of positive or negative trends among the seasons has been noticed. In winter (Fig. 11a), a similar spatial distribution than the yearly maximum H_s values has been observed, particularly for the negative trends with a maximum negative trend value equal to −0.28 m/10 years and identified in the southern area of the Tyrrhenian Sea. Conversely, positive trends ranging from 0 to 0.2 m/10 years were detected in some wave nodes in the Levantine, Ionian, Aegean and Balearic seas where the highest magnitude (0.13 m/10 year) has been identified. During spring (Fig. 11b), the spatial distribution of positive or negative trends was quite different from that observed in winter. In fact, positive trends with a peak value equal to 0.16 m/10 years mainly occurred in the western-central area of the Mediterranean Sea, including the Alboran, Balearic, Algerian and Tyrrhenian seas, while negative trends up to −0.13 m/10 years were identified in some wave nodes belonging to the western part of the Levantine basin. In summer, as opposed to the previous months, the highest positive trends, i.e. between 0.1 and 0.2 m/10 years, were concentrated in the central area of the Algerian Sea and in the Ionian Sea, near the Libyan coast, with a maximum magnitude equal to 0.17 m/10 years (Fig. 11c). Negative trends were detected in the western-central area of the Levantine basin, with an extreme value corresponding to −0.09 s/10 years (Fig. 11c). In autumn (Fig. 11d), the highest positive trend magnitude for the maximum seasonal H_s values occurred. This value was equal to 0.21 m/10 years, and has been observed in the northern area of the Algerian Sea and, specifically, close to the island of Corsica. Negative trends of about −0.2 m/10 years were instead concentrated in the western zone of the Levantine Sea.

Paying attention to the annual and seasonal maximum T_e values, the results deduced from the trend analysis are illustrated in Fig. 12 and Fig. 13, respectively. In particular, Fig. 12a highlights the percentages of grid points presenting positive or negative trends. As a result, at annual scale, a less marked positive trend has been identified when compared to the results obtained for the annual mean T_e values. Indeed, only 30.2% of the wave data showed a significant positive trend. Conversely, the percentage of significant negative trends was very low and equal to 0.2%.

Based on the trend analysis, the resulting spatial assessment for the yearly maximum T_e values is described in Fig. 12b. Positive trends occurred in various areas of the Mediterranean basin and, specifically, along the Balearic and Ligurian seas, in the northern parts of the Adriatic Sea, near the Tunisian coasts and especially in the Ionian basin with a maximum magnitude of 0.43 s/10 years. A negative trend of −0.05 s/10 years emerged only for one node in the Tyrrhenian Sea.

Also at seasonal scale, a marked reduction of significant positive trends passing from mean to maximum T_e values was generally noticed (Fig. 12a). In winter, a percentage of grid points equal to 19.2% and 0.2% showed significant positive and negative trends, respectively. During spring, an increase in the maximum T_e values has been detected in 39.9% of the grid points, while 0.5% of the grid points showed an opposite behaviour. In summer (72.8%), and in autumn (68.8%) the majority of the grid points evidenced a positive trend of the maximum T_e values, while the percentage of grid points with significant negative trends was very low and equal to 0.2% for both the seasons.

From a spatial point of view, during winter (Fig. 13a), positive trends of maximum T_e values were detected in few parts of the Mediterranean basin, especially close to the coastal areas. In particular, increment greater than 0.2 s/10 years were concentrated in the Balearic, Ligurian, Adriatic and Ionian seas, with a maximum value of 0.4 s/10 years corresponding to a wave node located in the northern part of the Ionian Sea. Concerning the spring season (Fig. 13b), the highest positive trend was equal to 0.40 s/10 years and was observed in the Ligurian Sea, while in only two wave nodes in the Aegean Sea negative trends have been detected, with a peak value equal to −0.1 s/10 years. In summer (Fig. 13c), a marked positive trend has been highlighted particularly in the Balearic and Ionian seas where, very close to the western Greek coast, the highest value of 0.37 s/10 years has been detected. A negative trend was observed in only one node placed in the Aegean basin, with a value equal to −0.04 s/10 years. During autumn (Fig. 13d), the highest positive trends were detected in the western-central zone of the Mediterranean Sea, especially in the Alboran (0.43 s/10 years), Balearic and Ligurian seas. As in the case of summer, only one node in the Aegean Sea evidenced a negative trend, equal to −0.09 s/10 years.

Results of the trend assessment of the annual and seasonal maximum

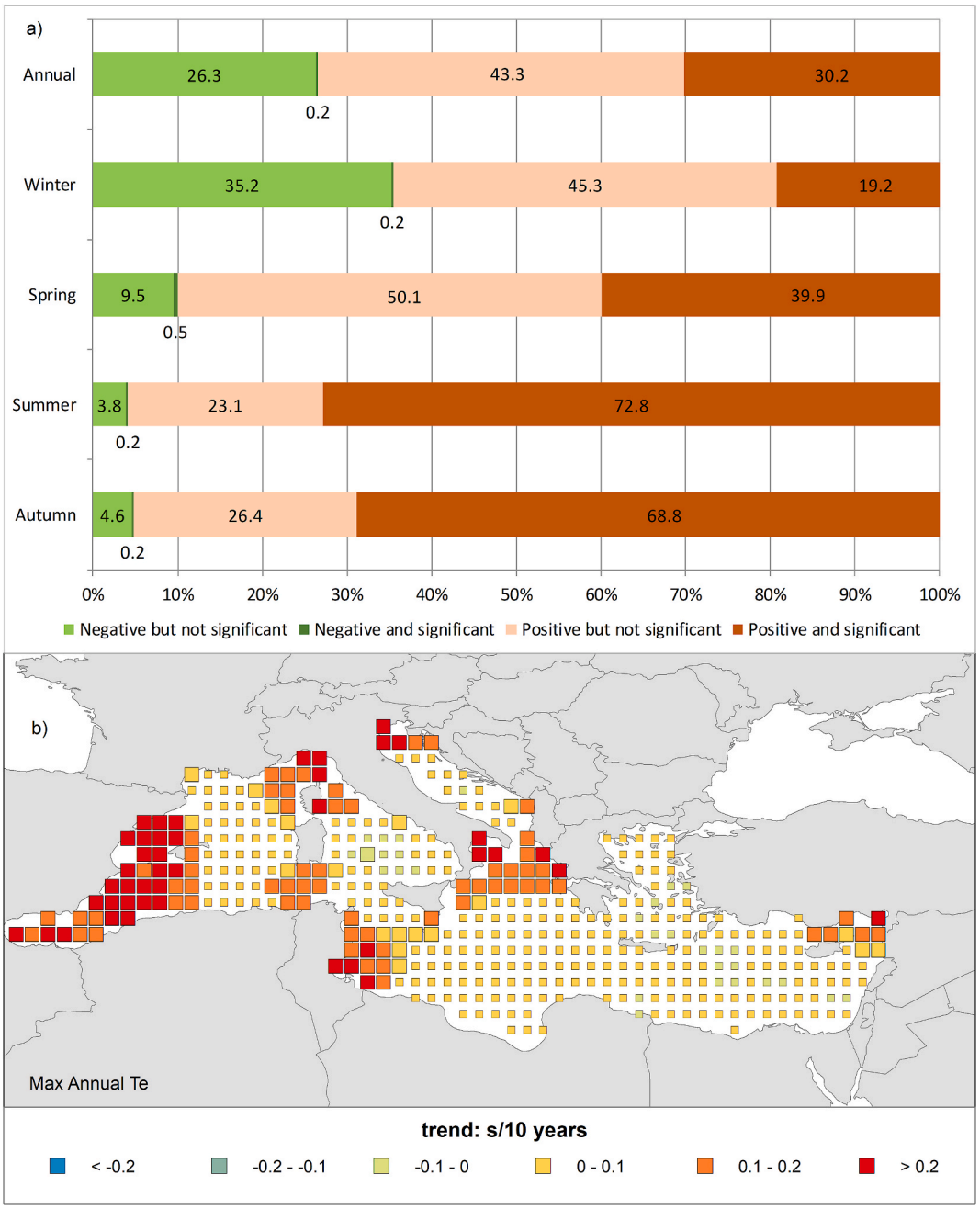

Fig. 12. (a) Seasonal and annual percentages of grid points presenting positive or negative trends in the T_e maximum values and (b) spatial distribution of the annual trend of maximum T_e.

P values are shown in Fig. 14 and Fig. 15. As regards the percentage of grid points showing positive or negative trends in the annual maximum *P* values (Fig. 14a), only 5.6% and 4.1% of the wave nodes evidenced positive and negative trends, respectively.

The spatial distribution of the trends related to the annual maximum *P* values is shown in Fig. 14b. Positive trends, between 5 and 10 kW/m/10 years, were mainly detected in some grid points belonging to the Algerian Sea, with a peak value equal to 9.94 kW/m/10 years. Negative trends with magnitude ranging from −10 to 0 kW/10 years, were individuated in one node near the southern coast of Sicily and in the Tyrrhenian Sea where a maximum negative value was equal to −9.97 kW/m/10 years has been identified.

The percentages of grid points with positive or negative trends at seasonal scale regarding the maximum *P* values are illustrated in Fig. 14a. The percentages of significant positive trends was lower than that detected for the mean *P* values. Specifically, 8.1%, 17%, 34.8% and 31.7% of the wave nodes showed increasing trends during winter, spring, summer and autumn, respectively. Conversely, a rise in the significant negative trends in comparison with those noticed for the mean *P* values was detected during all the seasons. In fact, negative tendencies were evidenced in 7.1%, 1.5%, 6.5% and 8.4% of the grid points for winter, spring, summer and autumn, respectively. The large variability of *P* values is due to the combination of H_s and T_e, based on equation (5).

The spatial distribution of the trends linked to the seasonal maximum *P* values is illustrated in Fig. 15. A marked variability among the seasons, and a general difference with the trend distribution detected for the seasonal mean *P* values, were observed. Due to its quadratic dependency on H_s, the present spatial behaviour resembles the one observed for the seasonal extreme H_s values (see Fig. 11). In winter (Fig. 15a), positive

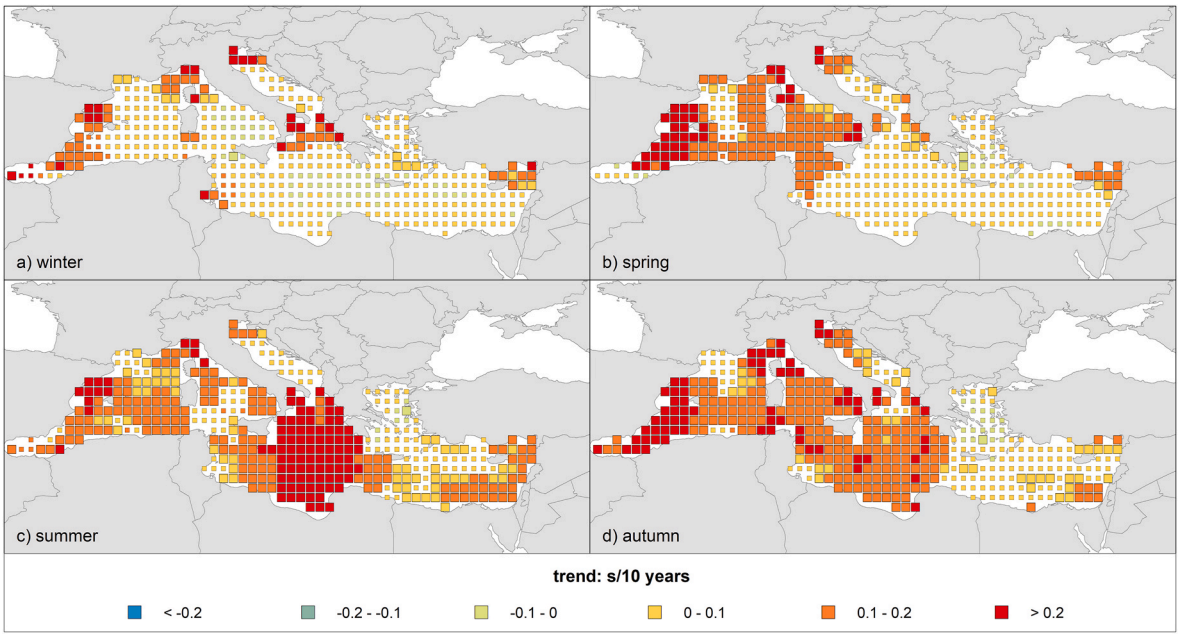

Fig. 13. Spatial distribution of the seasonal trend of the maximum T_e values for (a) winter, (b) spring, (c) summer and (d) autumn.

trends were detected in some areas of the Balearic, Ionian, Aegean and Levantine seas, with a maximum value equal to 4.8 kW/m/10 years and observed in the Balearic basin. Negative trends were instead detected between Sicily and Libya and in the Tyrrhenian Sea were the maximum reduction of −13.03 kW/m/10 years has been identified. A different spatial distribution was observed in spring when compared to the winter season (Fig. 15b), with a larger occurrence of positive trends in the western-central area of the Mediterranean basin and the eastern part of the Levantine Sea. The maximum positive trend was equal to 7.09 kW/m/10 years and was detected in the northern part of the Algerian Sea, close to the Corsica Island. Concerning the negative trends, they were concentrated in the western area of the Levantine Sea, with a maximum reduction of −3.69 kW/m/10 years. In summer (Fig. 15c), a maximum positive trend value equal to 5.17 kW/m/10 years has been detected in the Algerian Sea. Negative trends, instead, were observed in the Alboran Sea and in the central zone of the Levantine Sea with a maximum reduction of −1.15 kW/m/10. As shown in Fig. 15d, the autumn season was characterized by the highest percentage of positive trends with respect to the other seasons. These trends were principally detected in the Algerian and Ionian seas, with a maximum increase equal to 9.22 kW/m/10 years located in the southern part of the Algerian Sea. Similarly to the summer season, the negative trends in autumn were concentrated in the Levantine Sea, with a peak value equal to −5.98 kW/m/10 years.

5. Discussion

In this Section, a discussion of the obtained results on the wave trends in comparison with literature studies was performed.

With reference to the Eastern Mediterranean, involving the Ionian, Aegean and Levantine seas, the present findings related to the trends of mean wave parameters, with the exception of the Aegean basin, were different from that observed by Musić and Nicković (2008) who detected negative trends in the 50th percentile of H_s. The obtained results, instead, substantially agree with the ones obtained by Martucci et al. (2010) and Pomaro et al. (2017), who analysed the temporal evolution H_s for the Italian seas evaluated from different wave datasets in the periods 1958–1999 and 1979–2015, respectively. In particular, Martucci et al. (2010) evidenced an increasing trend in the yearly mean H_s series starting from 1989, while Pomaro et al. (2017) highlighted an increase in the 50th percentile of H_s. The analyses performed at a global scale by Young et al. (2011) revealed a positive trend on average H_s series in the most part of the Mediterranean Sea, with exclusion of some limited zones belonging to the Ionian, Ligurian, Levantine and Aegean seas. The obtained positive trends on mean H_s values also agreed with those obtained by De Leo et al. (2020) with reference to the Algerian and Ionian seas and the western area of the Levantine Sea, while they were in contrast in some areas such as the Ligurian Sea and the eastern part of the Levantine basin.

With reference to H_s, the comparisons with the current results at a seasonal scale were limited to the analysis of Casas-Prat and Sierra (2013) in the Balearic Sea and the Gulf of Lion for summer and winter, and of Pomaro et al. (2017) in a unique point belonging to the Northern area of the Adriatic Sea. Both the former work and the present modeling reveal a prevalence of positive trends and, conversely, an occurrence of negative trends in some scattered areas. As in the latter study, the present analysis also evidenced an increase in the 50th percentile of H_s in all seasons.

The results obtained by the current analysis with reference to the trends of yearly maximum values of H_s were similar with those observed by Musić and Nicković (2008) in the Eastern Mediterranean where slightly positive and negative trends appeared in the 90th and 99th percentile. Considering the whole Mediterranean Sea, Young et al. (2011) highlighted an overall positive trend in the 99th percentile of H_s at yearly scale, which substantially disagrees with the results obtained here, except for some areas belonging to the Adriatic, Ligurian, Algerian and Levantine seas. This discrepancy could be due to a coarse spatial resolution of the input database (2° × 2°). For the northern Adriatic Sea, where positive trends on the annual and seasonal maximum values of H_s were noticed, Pomaro et al. (2017), instead, detected overall negative trends considering the 95th and the 99th percentile, but using a temporal aggregation of 3 h. De Leo et al. (2020) analysed the yearly maximum H_s in the entire Mediterranean basin using hourly wave data with a spatial resolution of about 0.1° × 0.1°. Results showed a high percentage of not significant trends, as in the present study, with a general decreasing trend in the Tyrrhenian Sea, and in some zones of the Ionian, Adriatic and Levantine seas, not detected in this work. Moreover, as in the current analysis, positive trends were detected in the northern Adriatic Sea and in the Ligurian and Levantine seas, while those related in the Balearic and Aegean Sea were here not detected.

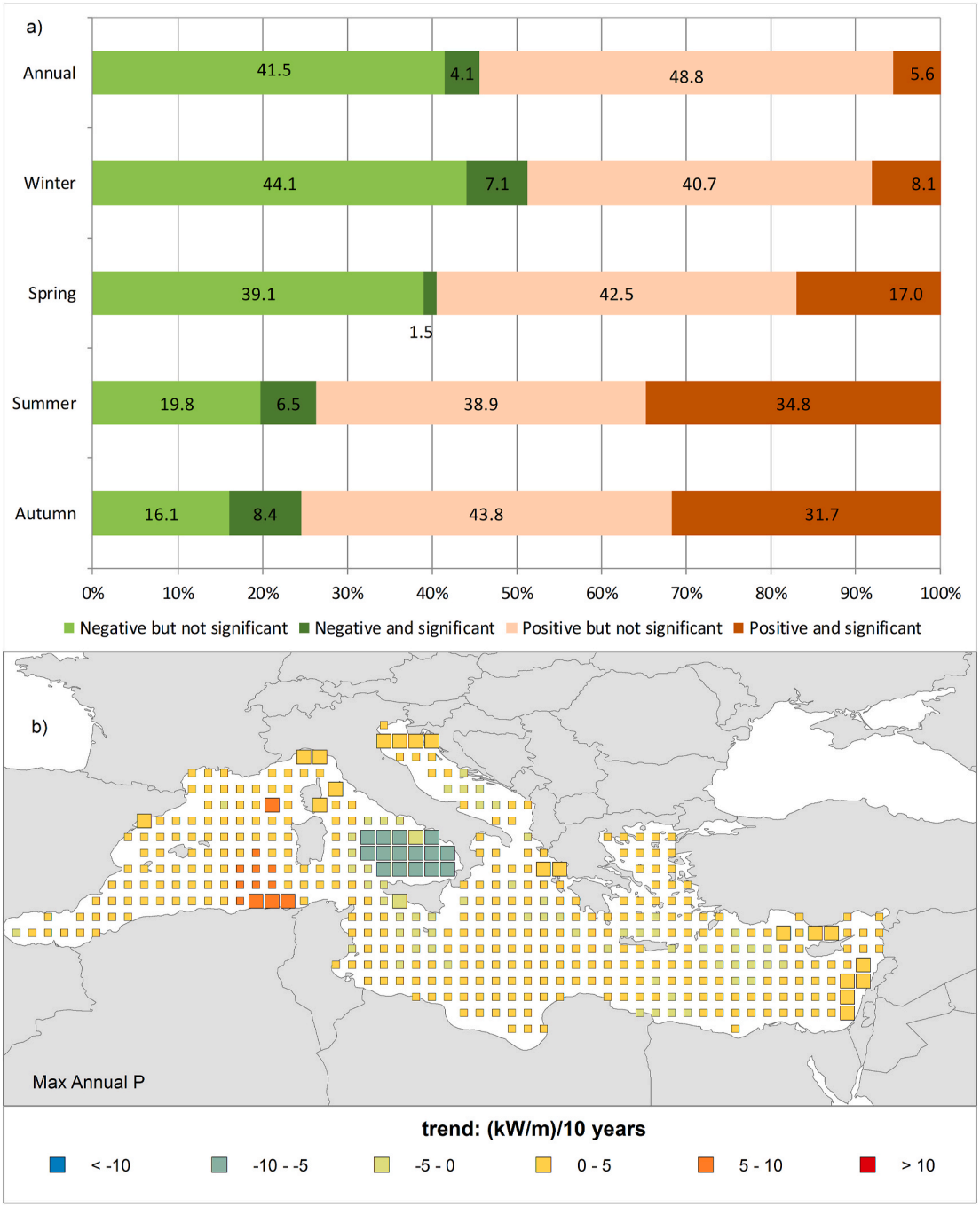

Fig. 14. (a) Seasonal and annual percentages of grid points presenting positive or negative trends in the *P* maximum values and (b) spatial distribution of the annual trend of maximum *P*.

In order to better appreciate the results of this study, an important remark must be made concerning some uncertainty issues. In fact, reanalysis data, such as the ERA-Interim, because of some advantages such as coverage, availability and costs are largely used in research studies. However, they should only be used with a proper understanding of their limitations and uncertainties (Tarek et al., 2020). Indeed, uncertainty estimation help understand the relative accuracy of the data, thus allowing to identify the areas or the periods where the products are thought to be less or more reliable (such as for recent dates compared to 30 years ago when fewer observations were available). Unfortunately, an uncertainty estimate has not been provided for the ERA-Interim and, thus, the results of this study are characterized by the uncertainties associated with random error (e.g., Hersbach et al., 2020). In fact, the uncertainty estimates mostly account for random errors and not for systematic ones. In order to overcome such a problem, the new reanalysis dataset ERA5 by the ECMWF includes information about uncertainties for all variables at reduced temporal resolutions (Hersbach et al., 2020).

6. Conclusions

A statistical trend analysis of mean and maximum values of significant wave height, energy period and wave power at yearly and seasonal scale has been conducted in the Mediterranean basin. To perform this analysis, a 40-year long time series, obtained through the global atmospheric reanalysis ERA-Interim by the ECMWF, has been used. The

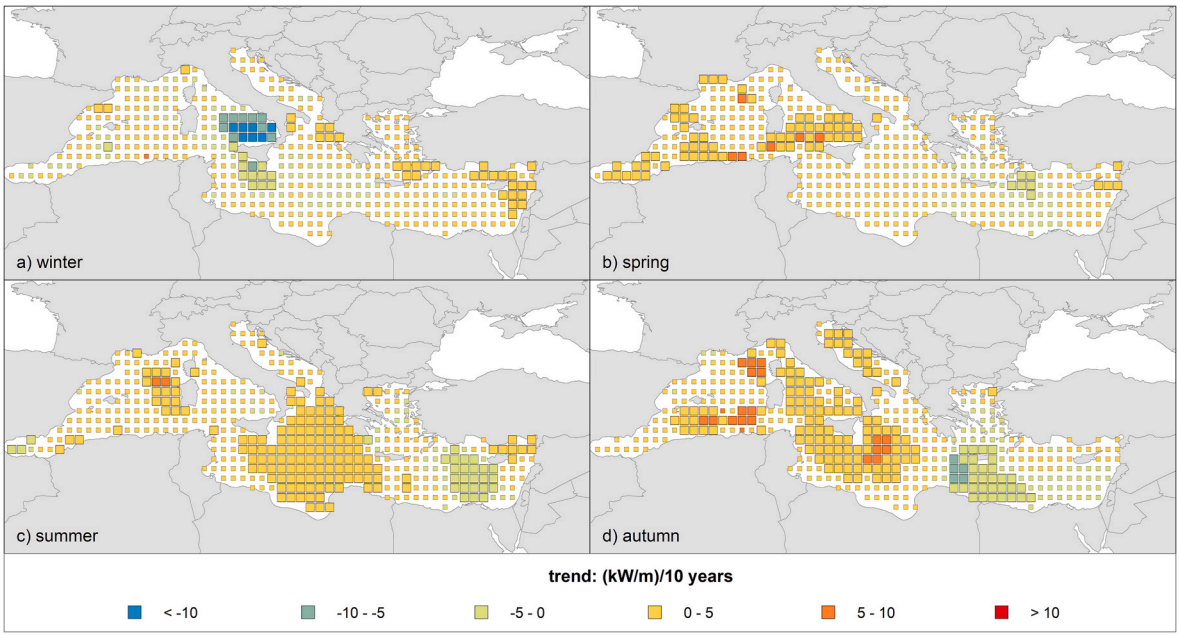

Fig. 15. Spatial distribution of the seasonal trend of the maximum P values for (a) winter, (b) spring, (c) summer and (d) autumn.

Mann-Kendall nonparametric test has been applied to detect possible trends at yearly and seasonal scales. The quantification of the magnitude of positive or negative trends has been carried out through the Theil-Sen estimator.

Concerning the trends of the mean values, the obtained results showed a general increase in the involved wave quantities at annual scale, mainly detected in the Algerian and Ionian seas. This positive trend was particularly evident for the energy period. The significant wave height was instead the quantity with the greatest trend variability. A decrease in significant wave height and wave power was observed in a limited area of the Aegean Sea. On a seasonal scale, positive trends were detected on the majority of the wave nodes. The highest increases of the significant wave height have been obtained during spring and autumn, and principally detected in the southern zone of the Mediterranean basin. Concerning the energy period, increases were spatially distributed in all seasons, while positive trends of the wave power were mainly observed during spring, summer and autumn. Paying attention to the results obtained by the trends of maximum values, a different feature was observed when compared to the analysis of the mean values. Indeed, significant trends of the considered three wave parameters were restricted to small zones of the Mediterranean basin, especially at yearly scale. However, the percentage of positive trends overcomes that of negative ones, which have been substantially detected in the Tyrrhenian and Levantine seas. The energy period represents the wave parameter with the highest percentage of significant trends. Considering the seasonal analysis, the trend variability among the seasons proved to be high, particularly for the significant wave height and the wave power.

The resulting analyses on H_s, T_e and P can have a relevant impact on different operations in various areas belonging to the Mediterranean Sea. The possible increase in future of the mean values could lead to an increase in coastal vulnerability with a resulting long-term shoreline retreat (e.g., Martins et al., 2017). Simultaneously, the positive trend of mean values of P can offer an improvement of the performance of WECs (e.g., Aristodemo and Algieri Ferraro, 2018). However, the inter-annual and seasonal variability of the mean values of P should be considered. Indeed, the area with the highest wave power, i.e. the Algerian Sea, is affected by a moderate inter-annual and seasonal variability which can influence the optimal extraction of the wave power over the year. The other area with a consistent wave power, i.e. the central zone of the Ionian Sea, is subject to a significant seasonal variability, with potential negative implications for a stable extraction of the wave energy. Owing to the small inter-annual and seasonal variability, the western part of the Levantine Sea and the Ligurian Sea can be considered good locations for future WEC installations.

Conversely, the small increase of maximum wave parameters, except for some isolated areas in the Mediterranean basin, weakly influences the magnitude of the design waves and then the sizing of offshore and coastal structures, and also the occurrence of coastal flooding due to extreme sea storms (e.g., Foti et al., 2020).

Further analyses will be dedicated to investigate trends of mean and maximum values of H_s, T_e and P in the Mediterranean basin at a higher space-time resolution with respect to the present wave dataset. In particular, wave databases such as ERA5 by ECMWF (e.g., Hersbach et al., 2020) and that provided by the hindcasting service of the University of Genoa (e.g., Mentaschi et al., 2015) will be considered.

CRediT authorship contribution statement

Tommaso Caloiero: Conceptualization, Methodology, Formal analysis, Software, Writing – original draft, Writing – review & editing, Visualization. **Francesco Aristodemo:** Conceptualization, Methodology, Formal analysis, Writing – original draft, Writing – review & editing. **Danilo Algieri Ferraro:** Data curation.

Declaration of competing interest

The authors declare that they have no known competing financial interests or personal relationships that could have appeared to influence the work reported in this paper.

Acknowledgments

The ECMWF wave data were obtained by the Meteorological Archival and Retrieval System (MARS) archive under the permission of the Italian Air Force.

Appendix A. Variability indicators for wave energy resource

The temporal variability of the wave power proves to be an important indicator to understand the feasibility of field installations of WECs. To investigate this aspect, the mean wave power at annual and seasonal scales was considered in order to calculate two important metrics: the coefficient of variation (*CV*) and the seasonal variability index (*SV*) (Cornett, 2008). The first one allows to determine the amount of variability of *P* with respect to its average value as follows:

$$CV = \frac{\sigma_P}{P_{mean}} \tag{A.1}$$

where σ_P represents the standard deviation of the mean annual wave power P_{mean}.

Values of $CV = 0$ mean the absence of variability, while values of $CV = 1$ mean that the standard deviation equals the average. Figure A1 shows the spatial distribution of the coefficient of variation of the mean annual *P* values. In the investigated area, the values of *CV* oscillate about between 0.08 and 0.3. This analysis allows to identify the areas more affected by the inter-annual variability. They substantially refer to the central Tyrrhenian Sea and the northern area of the Adriatic and Ionian seas, which are characterized by an overall low P_{mean}, also due to their proximity to the coasts. The lowest inter-annual variability is linked to the Alboran Sea, the northern part of the Algerian Sea, the western part of the Levantine Sea and below the Strait of Sicily. The areas characterized by high values of P_{mean}, i.e. Algerian Sea and the central part of the Ionian Sea, highlight values of *CV* ranging from 0.1 to 0.15.

The second metric considered in this study is the seasonal variability index which represents the rate of variation of *P* on a seasonal basis. This parameter is evaluated as:

$$SV = \frac{P_{S,max} - P_{S,min}}{P_{mean}} \tag{A.2}$$

where $P_{S,max}$ and $P_{S,min}$ are the mean wave powers for the most and the least energetic seasons.

Figure A2 describes the spatial distribution of the season variability index of the mean *P* values. It emerges that winter always represents the most energetic season, while the least energetic one is summer for about 90% of the grid points and spring for remaining grid points, mainly placed in the Aegean Sea and in the southern area of the Ionian Sea. The values of *SV* range about from 0.6 to 1.7. In this case, the most variable areas, i.e. highest *SV*, are associated to the central and southern Ionian Sea. The Alboran Sea is the portion of the Mediterranean basin with the lowest *SV*. The zone with the highest P_{mean}, i.e. the Algerian Sea, is characterized by a moderate seasonal variability, with values of *SV* just greater than 1.

The obtained results on *CV* and *SV* prove to be quite comparable in terms of magnitude and spatial location with those determined through different hindcast datasets by Besio et al. (2016) at the Mediterranean scale and by Liberti et al. (2013) along the Italian seas.

Appendix B. Correlations between the wave parameters

The correlations between the involved three wave parameters is here analysed in terms of the Pearson correlation coefficient considering two variable at a time, namely H_s and T_e, H_s and *P*, and T_e and *P*. The analysis was carried out through the mean and maximum values of the wave parameters at yearly scale.

Given a pair of generic variables *X* and *Y*, the Pearson correlation coefficient (CC) is evaluated as:

$$CC = \frac{cov(XY)}{\sigma_X \sigma_Y} \tag{B.1}$$

where *cov*(*XY*) is the covariance between the two variables, while σ_X and σ_Y are respectively the standard deviations of *X* and *Y*.

Figure B1 shows the spatial distribution of Pearson correlation coefficient between the mean and maximum annual values of H_s and T_e, H_s and *P*, and T_e and *P*. As highlighted in Figure B1a, an overall good correlation between the mean values of H_s and T_e has been identified, especially in the Algerian and Ionian seas with CC larger than 0.9. A quite scattered distribution of CC has been found considering the maximum values of H_s and T_e, with greatest CC observed in the Aegean Sea and smallest CC observed along some grid points close to the coasts (Figure B1b). As expected, due to the quadratic dependency of *P* on H_s, a strong correlation has been detected among these two parameters for both the mean (CC higher than 0.70) and the maximum values (CC higher than 0.95) in the whole Mediterranean basin (see Figures B1c and d). Regarding the correlation between T_e and *P*, the values of CC are generally lower than those detected for *P* and H_s. The mean values of T_e and *P* are well correlated in the same locations observed for the corresponding values of H_s and T_e, even if with a lower value of CC, i.e. greater than 0.8 (Figure B1e). The correlation between the maximum values of T_e and *P* is quite similar in terms of magnitude and placement of that identified for the corresponding values of H_s and T_e (Figure B1f).

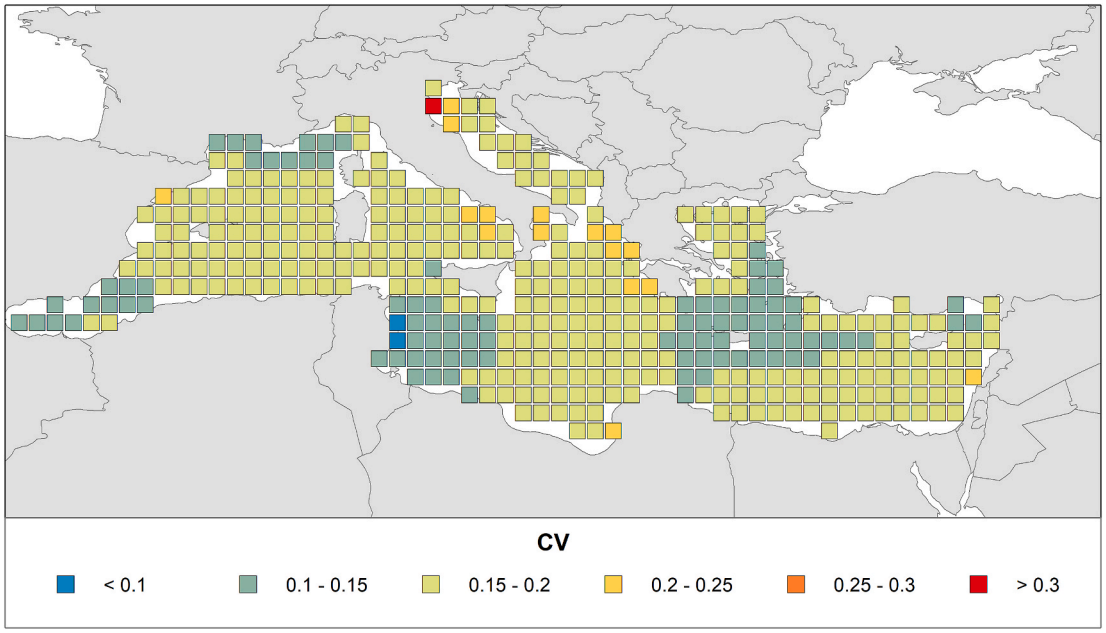

Fig. A.1. Spatial distribution of the coefficient of variation of the mean annual *P* values. .

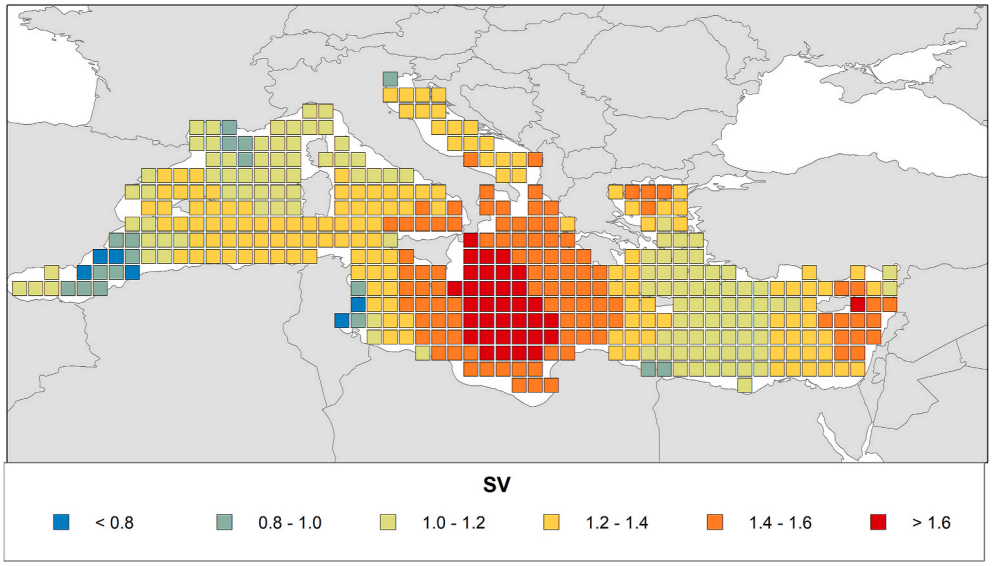

Fig. A.2. Spatial distribution of the seasonal variability index of the mean *P* values. .

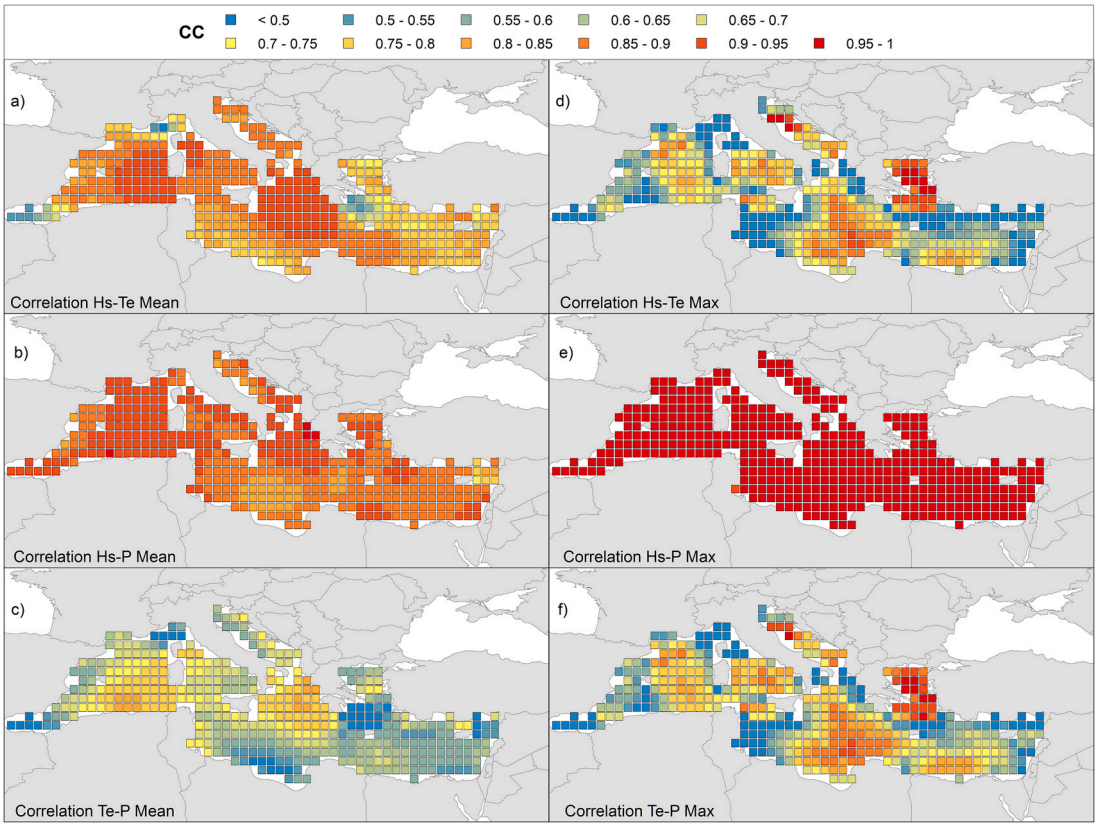

Fig. B.1. Spatial distribution of Pearson correlation coefficient between the mean annual values of (a) H_s and T_e (b) H_s and P (c) T_e and P and the maximum annual values of (d) H_s and T_e (e) H_s and P (f) T_e and P. .

References

Aarnes, O.J., Abdalla, S., Bidlot, J.R., Breivik, O., 2015. Marine wind and wave height trends at different ERA-Interim forecast ranges. J. Clim. 28, 819–837. https://doi.org/10.1175/JCLI-D-14-00470.1.

Algieri Ferraro, D., Aristodemo, F., Veltri, P., 2016. Wave energy resources along Calabrian coasts (Italy). Proc. of 35th International Conference on Coastal Eng., Antalya, Turkey 1–12. https://doi.org/10.9753/icce.v35.waves.5.

Amarouche, K., Akpınar, A., 2021. Increasing trend on storm wave intensity in the western mediterranean. Climate 9, 11. https://doi.org/10.3390/cli9010011.

Aristodemo, F., Algieri Ferraro, D., 2018. Feasibility of WEC installations for domestic and public electrical supplies: a case study off the Calabrian coast. Renew. Energy 121, 261–285. https://doi.org/10.1016/j.renene.2018.01.012.

Besio, G., Mentaschi, L., Mazzino, A., 2016. Wave energy resource assessment in the Mediterranean Sea on the basis of a 35-year hindcast. Energy 94, 50–63. https://doi.org/10.1016/j.energy.2015.10.044.

Caloiero, T., Aristodemo, F., Algieri Ferraro, D., 2019. Trend analysis of significant wave height and energy period in Southern Italy. Theor. Appl. Climatol. 138, 917–930. https://doi.org/10.1007/s00704-019-02879-9.

Caloiero, T., Aristodemo, F., 2021. Trend detection of wave parameters along the Italian seas. Water 13 (12), 1634. https://doi.org/10.3390/w13121634.

Casas-Prat, M., Sierra, J.P., 2013. Projected future wave climate in the NW Mediterranean Sea. J. Geophyis. Res. Oceans 118, 3548–3568. https://doi.org/10.1002/jgrc.20233.

Castelle, B., Dodet, G., Masselink, G., Scott, T., 2018. Increased winter-mean wave height, variability and periodicity in the Northeast Atlantic over 1949-2017. Geophys. Res. Lett. 45, 3586–3596. https://doi.org/10.1002/2017GL076884.

Chini, N., Stansby, P.K., 2012. Extreme values of coastal wave overtopping accounting for climate change and sea level rise. Coast. Eng. 65, 27–37. https://doi.org/10.1016/j.coastaleng.2012.02.009.

Clément, A., McCullen, P., Falcão, A., Fiorentino, A., Gardner, F., Hammarlund, K., Lemonis, G., Lewis, T., Nielsen, K., Petroncini, S., Pontes, M.T., Schild, P., Sjöström, B.O., Sørensen, H.C., Thorpe, T., 2002. Wave energy in Europe: current status and perspectives. Renew. Sustain. Energy Rev. 6 (5), 405–431. https://doi.org/10.1016/S1364-0321(02)00009-6.

Cornett, A., 2008. A Global Wave Energy Resource Assessment. Proc. Of 18th International Offshore and Polar Engineering Conference, ISOPE-I-08-370, Vancouver, USA, pp. 1–9.

Cramer, W., Guiot, J., Fader, M., et al., 2018. Climate change and interconnected risks to sustainable development in the Mediterranean. Nat. Clim. Change 8, 972–980. https://doi.org/10.1038/s41558-018-0299-2.

Dasgupta, S., Meisner, C., 2009. Climate Change and Sea Level Rise: A Review of the Scientific Evidence. Environment Department Papers, 118. Climate Change Series. World Bank, Washington.

De Leo, F., De Leo, A., Besio, G., Briganti, R., 2020. Detection and quantification of trends in time series of significant wave heights: an application in the Mediterranean Sea. Ocean. Eng. 202, 107155. https://doi.org/10.1016/j.oceaneng.2020.107155.

Foti, E., Musumeci, R.E., Stagnitti, M., 2020. Coastal defence techniques and climate change: a review. Rend. Fis. Acc. Lincei 31, 123–138. https://doi.org/10.1007/s12210-020-00877-y.

Galanis, G., Hayes, D., Zodiatis, G., Chu, P.C., Kuo, Y.H., Kallos, G., 2012. Wave height characteristics in the Mediterranean Sea by means of numerical modeling, satellite data, statistical and geometrical techniques. Mar. Geophys. Res. 33, 1–15. https://doi.org/10.1007/s11001-011-9142-0.

Giorgi, F., 2006. Climate change hot-spots. Geophys. Res. Lett. 33, L08707. https://doi.org/10.1029/2006GL025734.

González-Alemán, J.J., Pascale, S., Gutierrez-Fernandez, J., Murakami, H., Gaertner, M. A., Vecchi, G.A., 2019. Potential increase in hazard from mediterranean hurricane activity with global warming. Geophys. Res. Lett. 46, 1754–1764. https://doi.org/10.1029/2018GL081253.

Guillou, N., Chapalain, G., 2020. Assessment of wave power variability and exploitation with a long-term hindcast database. Renew. Energy 154, 1272–1282. https://doi.org/10.1016/j.renene.2020.03.076.

Gunn, K., Stock-Williams, C., 2012. Quantifying the global wave power resource. Renew. Energy 44, 296–304. https://doi.org/10.1016/j.renene.2012.01.101.

Hersbach, H., Bell, B., Berrisford, P., et al., 2020. The ERA5 global reanalysis. Q. J. Roy. Meteorol. Soc. 146, 1999–2049. https://doi.org/10.1002/qj.3803.

Hithin, N.K., Sanil Kumar, V., Shanas, P.R., 2015. Trends of wave height and period in the Central Arabian Sea from 1996 to 2012: a study based on satellite altimeter data. Ocean. Eng. 108, 416–425. https://doi.org/10.1016/j.oceaneng.2015.08.024.

IPCC, 2013. Summary for Policymakers. Fifth Assessment Report of the Intergovernmental Panel on Climate Change. Cambridge University Press, Cambridge and New York.

Kendall, M.G., 1962. Rank Correlation Methods. Hafner Publishing Company, New York.

Kumar, V.S., Joseph, J., Amrutha, M.M., Jena, B.K., Sivakholundu, K.M., Dubhashi, K.K., 2018. Seasonal and interannual changes of significant wave height in shelf seas around India during 1998–2012 based on wave hindcast. Ocean. Eng. 151, 127–140. https://doi.org/10.1016/j.oceaneng.2018.01.022.

Liberti, L., Sannino, G., Carillo, A., 2013. Wave energy resource assessment in the Mediterranean, the Italian perspective. Renew. Energy 50, 938–949. https://doi.org/10.1016/j.renene.2012.08.023.

Lionello, P., Cogo, S., Galati, M.B., Sanna, A., 2008. The Mediterranean surface wave climate inferred from future scenario simulations. Global Planet. Change 63, 152–162. https://doi.org/10.1016/j.gloplacha.2008.03.004.

Mann, H.B., 1945. Nonparametric tests against trend. Econometrica 13, 245–259. https://doi.org/10.2307/1907187.

Martins, K.A., de Souza Pereira, P., Silva-Casarín, R., Nogueira Neto, A.V., 2017. The influence of climate change on coastal erosion vulnerability in Northeast Brazil. Coast Eng. J. 59, 1740007. https://doi.org/10.1142/S0578563417400071.

Martucci, G., Carniel, S., Chiggiato, J., Sclavo, M., Lionello, P., Galati, M.B., 2010. Statistical trend analysis and extreme distribution of significant wave height from 1958 to 1999 - an application to the Italian Seas. Ocean Sci. 6, 525–538. https://doi.org/10.5194/os-6-525-2010.

Mentaschi, L., Besio, G., Cassola, F., Mazzino, A., 2015. Performance evaluation of wavewatch III in the Mediterranean Sea. Ocean Model. 90, 82–94. https://doi.org/10.1016/j.ocemod.2015.04.003.

Miche, M., 1951. Le Pouvoir Reflechissant des Ouvrages Maritimes Exposes a l'Action de la Houle. Annals des Ponts et Chaussess 12, 285–319.

Mitchell, T.D., Jones, P.D., 2005. An improved method of constructing a database of monthly climate observations and associated high-resolution grids. Int. J. Climatol. 25, 693–712. https://doi.org/10.1002/joc.1181.

Muraleedharan, G., Lucas, C., Guedes Soares, C., 2016. Regression quantile models for estimating trends in extreme significant wave heights. Ocean Eng. 118, 204–215. https://doi.org/10.1016/j.oceaneng.2016.04.009.

Musić, S., Nicković, S., 2008. 44-year wave hindcasting for the Eastern Mediterranean. Coast Eng. 55, 872–880. https://doi.org/10.1016/j.coastaleng.2008.02.024.

Neill, S.P., Hashemi, M.R., 2013. Wave power variability over the northwest European shelf seas. Appl. Energy 106, 31–46. https://doi.org/10.1016/j.apenergy.2013.01.026.

Pomaro, A., Cavaleri, L., Lionello, P., 2017. Climatology and trends of the Adriatic Sea wind waves: analysis of a 37–year long instrumental data set. Int. J. Climatol. 37, 4237–4250. https://doi.org/10.1002/joc.5066.

Portilla, J., Sosa, J., Cavaleri, L., 2013. Wave energy resources: wave climate and exploitability. Renew. Energy 57, 594–605. https://doi.org/10.1016/j.renene.2013.02.032.

Reguero, B.G., Losada, I.J., Méndez, F.J., 2015. A global wave power resource and its seasonal, interannual and long-term variability. Appl. Energy 148, 366–380. https://doi.org/10.1016/j.apenergy.2015.03.114.

Reguero, B.G., Losada, I.J., Méndez, F.J., 2019. A recent increase in global wave power as a consequence of oceanic warming. Nat. Commun. 10, 205. https://doi.org/10.1038/s41467-018-08066-0.

Shanas, P.R., Kumar, V.S., 2015. Trends in surface wind speed and significant wave height as revealed by ERA–Interim wind wave hindcast in the Central Bay of Bengal. Int. J. Climatol. 35, 2654–2663. https://doi.org/10.1002/joc.4164.

Sen, P.K., 1968. Estimates of the regression coefficient based on Kendall's tau. J. Am. Stat. Assoc. 63, 1379–1389. https://doi.org/10.1080/01621459.1968.10480934.

Shi, J., Zheng, J., Zhang, C., et al., 2019. A 39-year high resolution wave hindcast for the Chinese coast: model validation and wave climate analysis. Ocean Eng. 183, 224–235. https://doi.org/10.1016/j.oceaneng.2019.04.084.

Sierra, J.P., Casas-Prat, M., Campins, E., 2017. Impact of climate change on wave energy resource: the case of Menorca (Spain). Renew. Energy 101, 275–285. https://doi.org/10.1016/j.renene.2016.08.060.

Tarek, M., Brissette, F.P., Arsenault, R., 2020. Evaluation of the ERA5 reanalysis as a potential reference dataset for hydrological modelling over North America. Hydrol. Earth Syst. Sci. 24, 2527–2544. https://doi.org/10.5194/hess-24-2527-2020.

Ulazia, A., Penalba, M., Ibarra–Berastegui, G., Ringwood, J., Saénz, J., 2017. Wave energy trends over the Bay of Biscay and the consequences for wave energy converters. Energy 141, 624–634. https://doi.org/10.1016/j.energy.2017.09.099.

Vanem, E., Walker, S.E., 2013. Identifying trends in the ocean wave climate by time series analyses of significant wave height data. Ocean Eng. 61, 148–160. https://doi.org/10.1016/j.oceaneng.2012.12.042.

Vannucchi, V., Cappietti, L., 2016. Wave energy assessment and performance estimation of state of the art wave energy converters in Italian hotspots. Sustainability 8, 1300. https://doi.org/10.3390/su8121300.

Vicinanza, D., Contestabile, P., Ferrante, V., 2013. Wave energy potential in the north-west of Sardinia (Italy). Renew. Energy 50, 506–521. https://doi.org/10.1016/j.renene.2012.07.015.

Wang, S., McGrath, R., Hanafin, J., Lynch, P., Semmler, T., Nolan, P., 2008. The impact of climate change on storm surges over Irish waters. Ocean Model. 25, 83–94. https://doi.org/10.1016/j.ocemod.2008.06.009.

Weisse, R., von Storch, H., 2010. Marine Climate and Climate Changes: Storms, Wind Waves and Storm Surges. Springer Praxis Books in Environmental Sciences, Chichester, UK.

Xu, F., Perrie, W., 2012. Extreme waves and wave run-up in Halifax harbour under climate change scenarios. Atmos.-Ocean 50, 407–420. https://doi.org/10.1080/07055900.2012.707610.

Young, I.R., Zieger, S., Babanin, A.V., 2011. Global trends in wind speed and wave height. Science 332, 451–455. https://doi.org/10.1126/science.1197219.

Zheng, C., Zhang, R., Shi, W., Li, X., Chen, X., 2017. Trends in significant wave height and surface wind speed in the China Seas between 1988 and 2011. J. Ocean Univ. China 16, 717–726. https://doi.org/10.1007/s11802-017-3213-z, 2017.

Zikra, M., Ashfar, P., Mukhtasor, M., 2016. Analysis of wave climate variations based on Era-Interim reanalysis data from 1980 to 2014 to support wave energy assessment in Indonesia. ARPN J. Eng. Applied Sciences 11, 879–884.